JEFF NDW, Session Fusion, 25 Nov. 2024, EFFDOC-1547
(EUROfusion WPBB-S.05.02-T007 Monitoring meeting)
[https://www.oecd-nea.org/dbdata/nds_effdoc/effdoc-1547.pdf]

PNIII-P4-PCE-2021-1260

WPBB-S.05.02-T007-D004

Progress Report on neutron-induced alpha-emission analysis

**[EUROfusion WPBB-S.05.02-T007-D004:
Validation of the assessment of particular alpha-particle emission induced by fast neutrons on structural materials around 10 MeV]**

Vlad Avrigeanu and Marilena Avrigeanu
Horia Hulubei National Institute for Physics & Nuclear Engineering, (IFIN-HH), Bucharest, Romania

Content

1. **Introduction:** WPBB-S.05.02-T007-D004: **31.12.2024**
2. **Analysis of 2022 first data of ^{91}Zr(n,α)^{88}Sr reaction + (GQR) + %EWSR** [EFFDOC-1538(Apr.2024)]
   [accuracy/uncertainty]: PLB **858**(2024)139078
3. **EWSR systematics: (α,α'), (γ,α), (n,α) reactions:** PLB **858**(2024)139078
4. (n,α) ISGQR / EWSR vs. (a) Γ_{syst}**(2001),** and (b) **Lorentzian** ISGQR: PLB Suppl. material
5. **Conclusions:** 1. **Suitable (GQR+)DR+PE+CN account of alpha-particle emission confirmed**
   2. **EWSR systematics: 50-100% [(α,α')] vs. 100-10% [(x,α)], x=γ,n**

1. WPBB-S.05.02-T007-D004 Obj./Del. [https://ims.euro-fusion.org]

IFIN-HH

Task Specification (TS)

EUROfusion

[EFFDOC-1538(Apr.2024)]

TS Title:	Nuclear Data Evaluations - 2024		
TS Ref. Nr.:	BB-S.05.02-T007	Task coordinator:	Dieter Leichtle
Status:	In review	Date:	14-Feb-2024

D004: Technical Specification: Validation of the assessment of particular alpha-particle emission induced by fast-neutrons on structural materials around 10 MeV (IAP)

Further validation of the alpha-particle optical model potential (OMP) developed within F4E/EUROfusion deriverables, for a sound description of the alpha-emission in neutron-induced reactions, is needed due to most recent measurement and analysis of (n,α) reaction cross sections [e.g, Phys. Rev. C **106**, 064602 (2022) for 91Zr target nucleus]. Measured data larger by ~100% than actual evaluations (TENDL-2021/2023) led firstly to changes of the above-mentioned OMP (also the actual default option of the code-system TALYS-2.0 used to provide TENDL), however at variance with other recent measurements by wide collaborations (e.g., arXiv:2402.01534 [nucl-ex], 2 Feb 2024). Thus it becomes necessary and is proposed an additional analysis of these data as well as eventual role of the alpha-emission decay of nuclei excited just at the isoscalar Giant Quadrupole Resonance (GQR) energies within (n,α) reactions below and around the incident energy of 14 MeV. Former EUROfusion/WPBB similar analyses [Eur. Phys. J. A **57**, 54 (2021), **58**, 189 (2022), Phys. Rev. C **107**, 034613 (2023)] should and will be completed in this respect also by comparison of the corresponding Energy Weighted Sum Rule (EWSR) data with the available systematics

PM: 3 PM (IAP)

ID	Title	Start Date	End Date	RU	Del. Owner	AWP2024 PM 50% standard
BB-S.05.02-T007 - D004	Validation of the assessment of particular alpha-particle emission induced by fast-neutrons on structural materials around 10 MeV	01-Jan-24	31-Dec-24	IAP	Vlad Avrigeanu	3.000

2.1 α's OMP[1994/2003-2010/2014-2023] / α-emission

[EFFDOC-1538(Apr.2024)]

IFIN-HH

PHYSICAL REVIEW C **90**, 044612 (2014)

Further explorations of the α-particle optical model potential at low energies for the mass range $A \approx 45$–209

F4E-GRT-168.01-5.1

PHYSICAL REVIEW C **91**, 064611 (2015)

Consistent optical potential for incident and emitted low-energy α particles

F4E-GRT-168.02-8.1

Zn(p,α)

YES!

PHYSICAL REVIEW C **94**, 024621 (2016)

Analysis of uncertainties in α-particle optical-potential assessment below the Coulomb barrier

F4E-GRT-168.02-8.1

α-emission

PHYSICAL REVIEW C **96**, 044610 (2017)

Consistent optical potential for incident and emitted low-energy α particles. II. α emission in fast-neutron-induced reactions on Zr isotopes

PPPT-WPMAT-5.7.1-T001-D001

NO!!

Zr(n,α)

α-OMP setting/validation

PHYSICAL REVIEW C **99**, 044613 (2019)

Role of consistent parameter sets in an assessment of the α-particle optical potential below the Coulomb barrier

PPPT-WPMAT-7.1-T004-D001

PHYSICAL REVIEW C **106**, 024615 (2022)

Charged-particle optical potentials tested by first direct measurement of the $^{59}Cu(p, \alpha)^{56}Ni$ reaction

WPBB-S.05.02-T001-D018

PHYSICAL REVIEW C **107**, 034613 (2023)

Consistent optical potential for incident and emitted low-energy α particles. III. Nonstatistical processes induced by neutrons on Zr, Nb, and Mo nuclei

WPBB-S.05.02-T001-D005

$^{90,91,92}Zr(\alpha,\gamma)$, ^{96}Zr, $^{100}Mo(\alpha,n)$

frontiers | Frontiers in Physics

DOI 10.3389/fphy.2023.1247311

M. Avrigeanu* and V. Avrigeanu†

Constrained model assumptions using recent data of α-particle reactions on ^{144}Sm.

WPBB-S.05.02-T005-D007

$^{144}Sm(\alpha,\gamma)$

2.1 α's OMP[1994/2003-2010/2014-2023/2021-on] / α-emission / GQR

Eur. Phys. J. A (2021) 57:54
https://doi.org/10.1140/epja/s10050-020-00336-0
THE EUROPEAN PHYSICAL JOURNAL A

WPPMI-7.4-T004-D002

Validation of an optical potential for incident and emitted low-energy α-particles in the $A \sim 60$ mass range

Fe,Co,Cu,Zn(n,α) , (p,α)

α-emission YES!!! +DR+GQR

Eur. Phys. J. A (2022) 58:189
https://doi.org/10.1140/epja/s10050-022-00831-6
THE EUROPEAN PHYSICAL JOURNAL A

WPPMI-7.4-T004-D004

Validation of an optical potential for incident and emitted low-energy α-particles in the $A \sim 60$ mass range II. Neutron–induced reactions on Ni isotopes

Ni(n,α)

PHYSICAL REVIEW C 107, 034613 (2023)

WPBB-S.05.02-T001-D005

Consistent optical potential for incident and emitted low-energy α particles III. Nonstatistical processes induced by neutrons on Zr, Nb, and Mo nuclei

Zr,Nb,Mo(n,α)

frontiers | Frontiers in Physics
DOI 10.3389/fphy.2023.1142436

Consistent assessment of neutron-induced activation of ^{93}Nb

Nb(n,x)

WPBB-S.05.02-T005-D007

Phys. Lett. B 858 (2024) 139078
Contents lists available at ScienceDirect
Physics Letters B
journal homepage: www.elsevier.com/locate/physletb
ELSEVIER

WPBB-S.05.02-T007-D004

91Zr(n,α)88Sr +

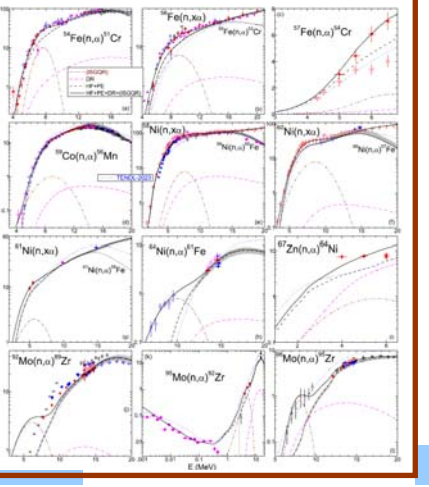

Letter

Giant quadrupole resonances within neutron-induced α-particle emission?

M. Avrigeanu, V. Avrigeanu,*
Horia Hulubei National Institute for Physics and Nuclear Engineering, 077125 Bucharest-Magurele, Romania

ARTICLE INFO

Editor: A. Schwenk

ABSTRACT

The particular conditions for the recent measurement of ^{91}Zr$(n,\alpha)^{88}$Sr reaction cross sections at incident energies

[DR+PE+CN *Consistent* model calculations (Method, Tools, IP)] (1/3)

[E.D. Arthur – P.G. Young, LANL, '80]

[EFFDOC-1518(Nov.2023)]+

YES

i. **unitary use of *common model parameters* for different mechanisms**

ii. **use of *consistent sets* of input parameters (IP) validated by *analyses of various independent* experimental data** (*e.g.*, other than activation)

iii. **unitary account of *whole body* of related experimental data for** *isotope chains* and ***neighboring elements***

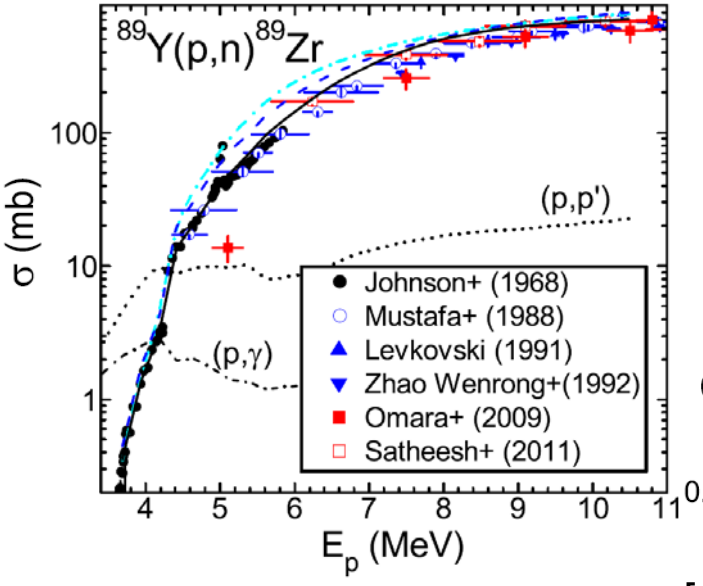

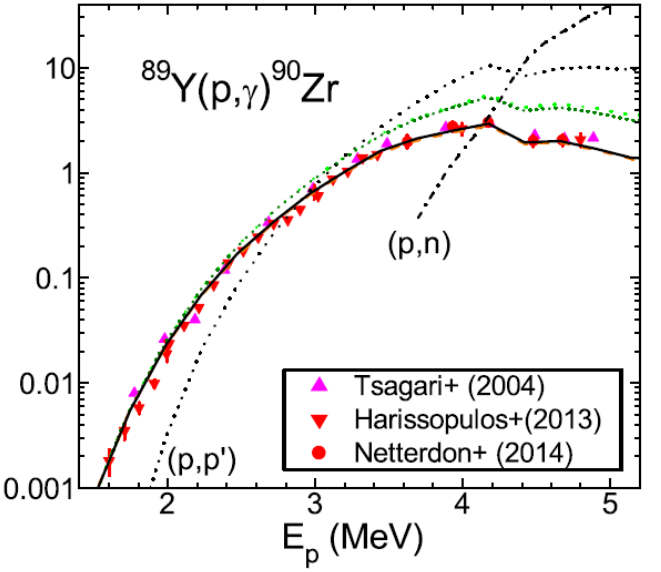

[PHYSICAL REVIEW C **96**, 044610 (2017)]

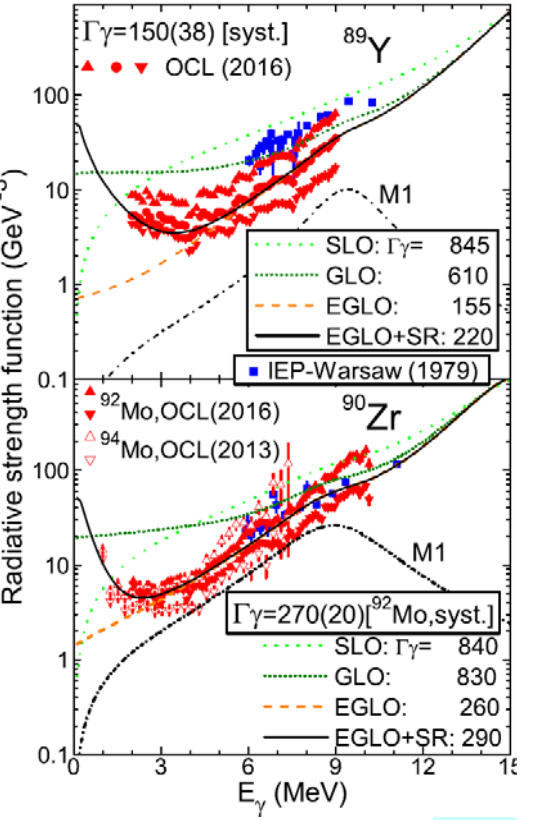

NO re-normalization or free parameters (widely-used within ND libraries)

[*Consistent* model calculations (Method, Tools, IP)] (2/3)

EFFDOC-1518(Nov.2023)+

OPTICAL MODEL : prime tool for all cross section calculations

- **Phenomenological OMP (global parameter sets): still extensively used**
- **Microscopic OPs: reduced uncertainties (e.g., OM ambiguities)**

- **Pure elastic scattering OP analysis**
  SCAT2 [O. Bersillon]
  - phenomenological OP
  + semi-microscopic (DF) OP
  (M. Avrigeanu - local version)

Phys. Rev. C **62** (2000) 017001
Nucl. Phys. A **693** (2001) 616
Eur. Phys. J. A **12** (2001) 399
Int. J. of Mod. Phys. E **11** (2002) 249
Nucl. Phys. A **723** (2003) 104
Nucl. Phys. A **759** (2005) 327
Nucl. Phys. A **764** (2006) 246

- **DWBA / Coupled Reaction Channel (CRC)**
  FRESCO-2003 [I.J. Thompson]: **(n,α), (p,α) PICK-UP**

- **Composite system equilibration**
  - **Geometry Dependent Hybrid** (GDH) preequilibrium-emission model
  - **Hauser-Feshbach** (HF) statistical model

  STAPRE-H95 [V. Avrigeanu, M. Avrigeanu] (updated)

- **Giant Quadrupole Resonance (GQR)** [PLB **613**,128 (2005), NPA **764**, 246 (2006)]
  - Gaussian: $E_{0,GQR}=64/A^{1/3}$ MeV (phenomenologically: Γ~1 MeV, σ~1 mb)
  [M.N. Harakeh and A. van der Woude, *Giant Resonances*, Oxford,2001]

[PE+CN *Consistent* model calculations (Method, Tools, IP)] (3/3)

IFIN-HH

[EFFDOC-1518 (Nov.2023)]+

LOCAL APPROACH:

STAPRE-H95 (updated-2020) [OM/PE/SM: SCAT2, GDH, HF]

- **n/p- spherical OMP:** Koning-Delaroche, Nucl.Phys. **A713**, 231 (2003)
- **α- spherical OMP:** V. Avrigeanu+, PRC **90**, 044612 (2014)
- **Nuclear-level density** (E>E_d [**ENSDF**]): **BSFG:** [DOI: 10.1103/PhysRevC.107.034613]
  - + **E*<S: (*a*,Δ) by fit** of **D0 (RIPL-3)** & **Nd (ENSDF,RIPL3)**
  - + **E*>S: *a*(E*)** [A.R. Junghans+, NP**A 629**, 635 (1998), A.J. Koning+, PRC **56**, 970 (1997)]
  - + l/l_r: 1/2(*gs*)-3/4(*S*)-1(15 MeV) [V.Avrigeanu+,JNST **S2**,746(2002); M.Avrigeanu+,PRC **85**, 044618 (2012)]

Fitted level and resonance data

Nucleus	N_d	E_d^* (MeV)	N_d	E_d^* (MeV)	$S+\frac{\Delta E}{2}$ (MeV)	I_0	D_0^{exp} [a] (keV)	a (MeV^{-1})	Δ (MeV)
^{88}Sr	47	4.801	47	4.801	11.113	9/2	0.29(8)	8.70	1.63
^{91}Zr	37	3.053	37	3.053	7.260	0	6.0(14)	9.77	0.40
^{92}Zr	42	3.500	54(2)	3.725	8.647	5/2	0.55(10)	9.67(27)(25)	0.79(9)(6)

[a]RIPL-3 [22] if not otherwise mentioned.

- **γ-ray strength functions:** E1 [EGLO/OCL: NDS **163**,109(2020), PRC **94**,025804(2016)] **[IAEA CRP-photonuclear];** M1 [SLO + upbend, PRC **94**, 025804 (2016)]
- **PE: Geometry Dependent Hybrid model** [M. Blann+, PRC **28**, 1493 (1984)]
  - + **J^π-conservation** [Z.Phys. A **329**,177(1988)]
  - + **$g_p(u)$~u, $A_K(p,h)$, $f_K(p,h,E,F_1(I,E_i)$** [Phys. Rev. C **58**, 295 (1998)], F=40 MeV
  - + **α-emission:** [Milano approach, ZPA **329**, 177 (1988)] replaced by **$g_\alpha=(6/\pi^2)a$**

2.2. Analysis of 2022 *first* (n,α) data/question (91Zr)

(1/2)

[EFFDOC-1518 (Nov.2023)]

PHYSICAL REVIEW C **106**, 064602 (2022)

Cross sections of the $^{91}Zr(n,\alpha)^{88}Sr$ reaction in the 3.9–5.3 MeV neutron energy region

Guohui Zhang,[1] E. Sansarbayar,[2,3,*] Yu. M. Gledenov,[2] G. Khuukhenkhuu,[3] L. Krupa,[4,5] N. S. Gustova,[4] M. G. Voronyuk,[4] I. Chuprakov,[2,6,7] N. Battsooj,[3] I. Wilhelm,[5] M. Solar,[5] R. Sykora,[5] Z. Kohout,[5] Jie Liu,[1] Yiwei Hu,[1] and Zengqi Cui[1]

[1]*State Key Laboratory of Nuclear Physics and Technology, Institute of Heavy Ion Physics, School of Physics, Peking University, Beijing 100871, China*

[2]*Frank Laboratory of Neutron Physics, Joint Institute for Nuclear Research, Dubna 141980, Russia*

[3]*Nuclear Research Center, National University of Mongolia, Ulaanbaatar 210646, Mongolia*

[4]*Flerov Laboratory of Nuclear Reactions, Joint Institute for Nuclear Research, Dubna 141980, Russia*

[5]*Institute of Experimental and Applied Physics, Czech Technical University in Prague, Husova 240/5, Prague 1, 110 00, Czech Re*

[6]*Faculty of Physics and Technology, L.N. Gumilyov Eurasian National University, Nur-sultan 010000, Kazakhstan*

[7]*The Institute of Nuclear Physics, Ministry of Energy of the Republic of Kazakhstan, Almaty 050032, Kazakhstan*

(Received 20 July 2022; accepted 17 November 2022; published 8 December 2022)

Cross sections of the $^{91}Zr(n,\alpha)^{88}Sr$ reaction were measured at four incident neutron energies in the range of 3.9 to 5.3 MeV. The experiment was carried out on the Van de Graaff accelerator EG- Laboratory of Neutron Physics, Joint Institute for Nuclear Research, Russia. Fast neutrons we the $^{2}H(d,n)^{3}He$ reaction with a deuterium gas target. A twin gridded ionization chamber (GIC) charged particle detector, in which ^{91}Zr back-to-back samples on a tantalum backing were placed cathode. The relative and absolute neutron fluxes were measured using two $^{238}U_3O_8$ samples Cross-section data obtained in this measurement were compared with those in existing data l theoretical calculations using TALYS code. The present data for the $^{91}Zr(n,\alpha)^{88}Sr$ reaction shou clarifying the discrepancies in various published nuclear evaluation data. An alpha clustering fac using the statistical model and knock-on mechanism.

(n,α_0) - cross sections measured

(n,α_1) - cross sections by TALYS

($n,\alpha_{0,1}$) – c.s. deduced

GUOHUI ZHANG *et al.*

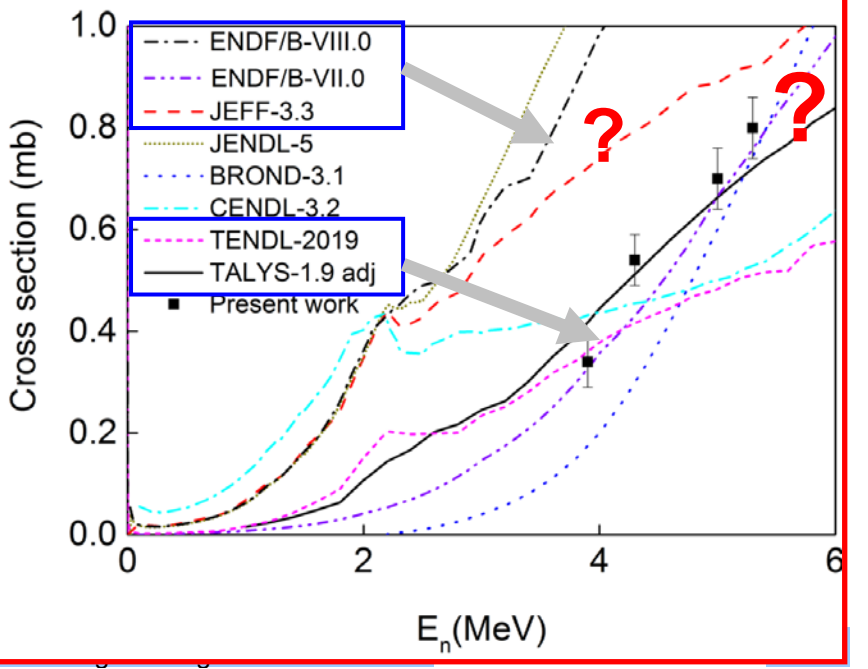

At variance with:

- PRC **107**, 034613 (2023): **$^{90\text{-}92,94,96}$Zr(n,x)**
  Avrigeanu+ (submitted: 21 Oct. 2022)
- PRC **34**, 2065 (1986): **^{90,91}Zr(n,α),** dσ/dE
  Gadioli+, En=14.3, 18.15 MeV,
  pick-up support !

Analysis of 2022 *first* (n,α) data on 91Zr

[EFFDOC-1538(Apr.2024)] (2/2)

IFIN-HH

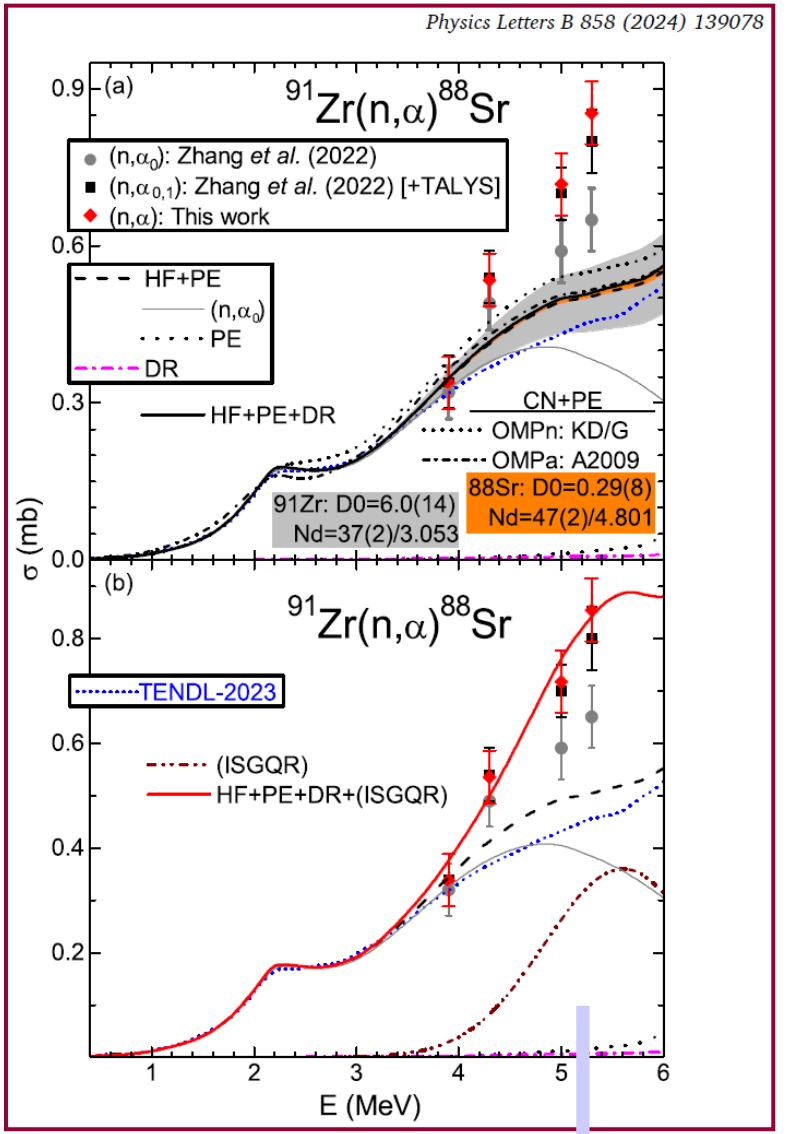

4.3(24) %EWSR !!!

+

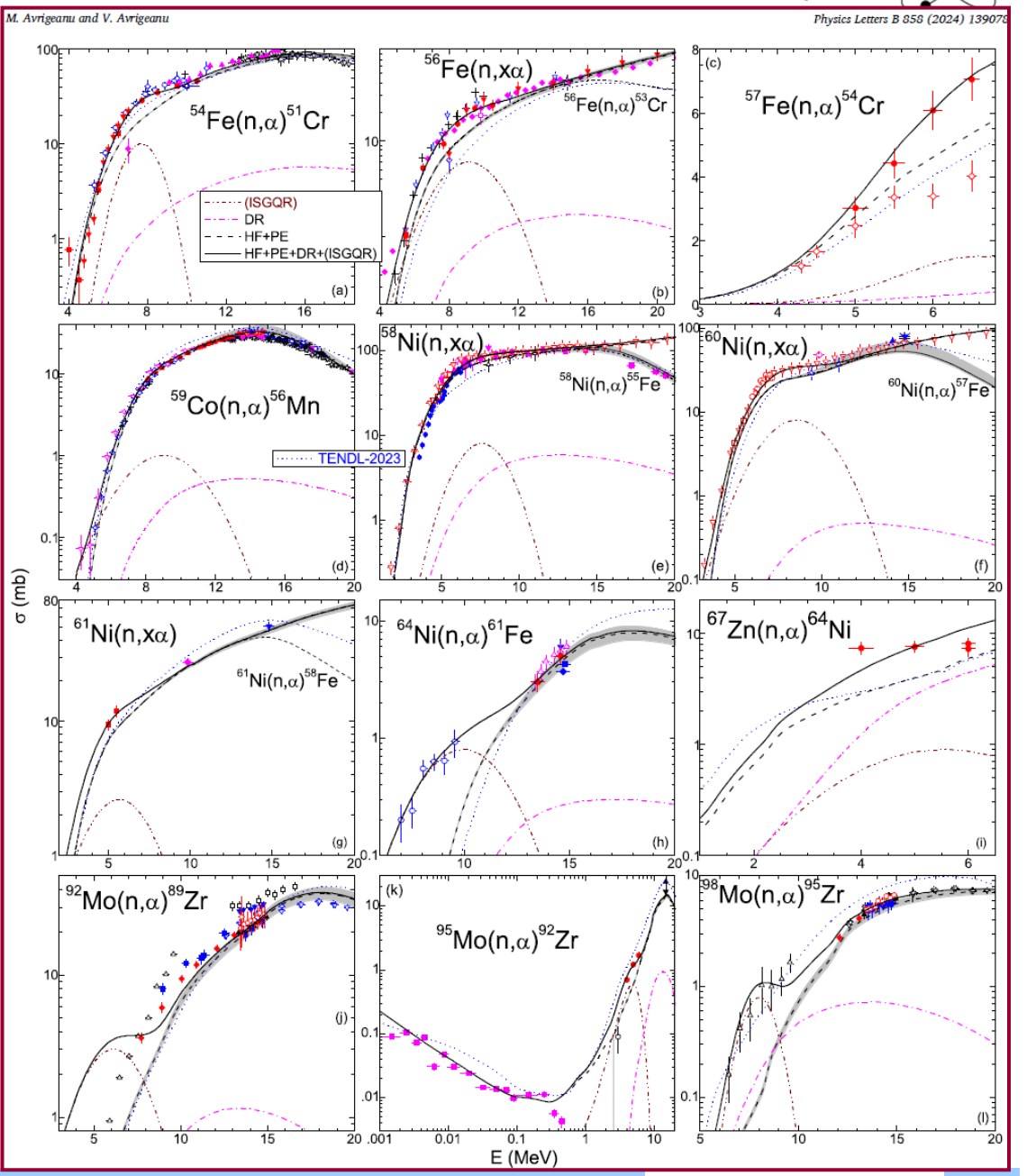

3. EWSR systematics: (α,α'), (γ,α), (n,α) reactions

(1/2)

[EFFDOC-1538(Apr.2024)]

ISGQR:

$$S_{-2}^{E2} = \int \sigma^{GQR} dE / E^2 = (1/E_0^2) \int \sigma^{GQR} dE$$

K. Raghunathan, L. L. Rutledge, R. E. Segel, and L. Meyer-Schützmeister, Phys. Rev. C **22**, 2409 (1980).

EWSR (energy weighted sum rule):

$$SR_{-2}^{E2} = 0.22 Z^2 A^{-1/3} \ \mu b/MeV$$

E. Kuhlmann, E. Ventura, J. R. Calarco, D. G. Mavis, and S. S. Hanna, Phys. Rev. C **11**, 1525 (1975),

Physics Letters B 858 (2024) 139078

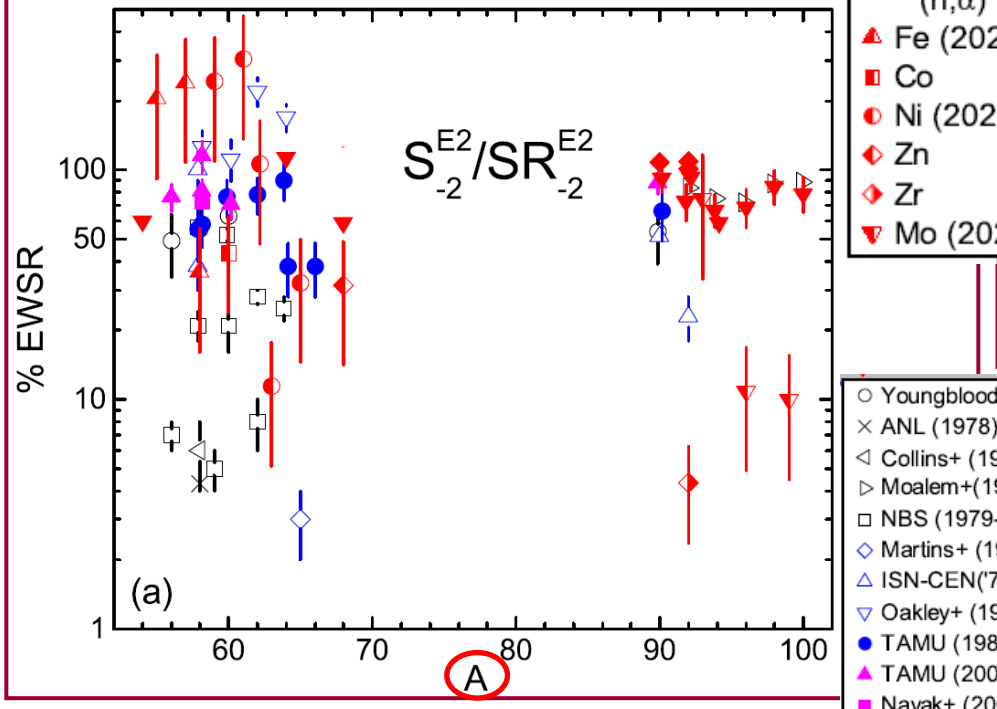

M. Avrigeanu and V. Avrigeanu

Table 1
The ISGQR energies [24] and the ISGQR-*like* peak cross sections and FWHM for neutron-induced α-emission (given in this work if not otherwise mentioned) and ISGQR Gaussian distribution, the corresponding integrated yields and ISGQR strength functions S_{-2}^{E2} as well as their EWSR fractions SR_{-2}^{E2}.

Excited nucleus	E_0 [24] (MeV)	σ_0 (mb)	Γ (MeV)	$\int \sigma^{GQR} dE$ (mb MeV)	S_{-2}^{E2} (μb/MeV)	($\%\, SR_{-2}^{E2}$)
^{55}Fe	16.829	10[a]	2.1[a]	22.6	79.7	204
^{57}Fe	16.630	6[a]	4[a]	25.6	92.5	239
^{58}Fe	16.534	1.5[a]	2.4[a]	3.76	13.8	35.8
^{60}Co	16.348	1	4.5	4.8	17.8	43.5
^{59}Ni	16.440	8[b]	3.4[b]	29.1	108	243
^{61}Ni	16.258	8[b]	4.1[b]	35.1	133	303
^{62}Ni	16.170	2.6[b]	4.4[b]	12.1	46.1	106
^{63}Ni	16.084	0.3[b]	4[b]	1.28	4.9	11.4
^{65}Ni	15.918	0.8[b]	4.1[b]	3.51	13.9	32.3
^{68}Zn	15.680	0.9	3.9	3.76	15.3	31.5
^{92}Zr	14.177	0.36	1.8	0.68	3.4	4.3
^{93}Mo	14.126	3[c]	4[c]	12.8	64.1	74.8
^{96}Mo	13.977	0.6[c]	2.8[c]	1.81	9.2	10.9
^{99}Mo	13.835	0.8[c]	1.9[c]	1.6	8.4	10

[a] Ref. [13], with eventual minor changes due to slightly different ISGQR energies [24,27] (including an improved account for the excited nucleus ^{57}Fe).
[b] Ref. [14], as above.
[c] Ref. [8], as above.

3. EWSR systematics: (α,α'), (γ,α), (n,α) reactions

[EFFDOC-1538(Apr.2024)]

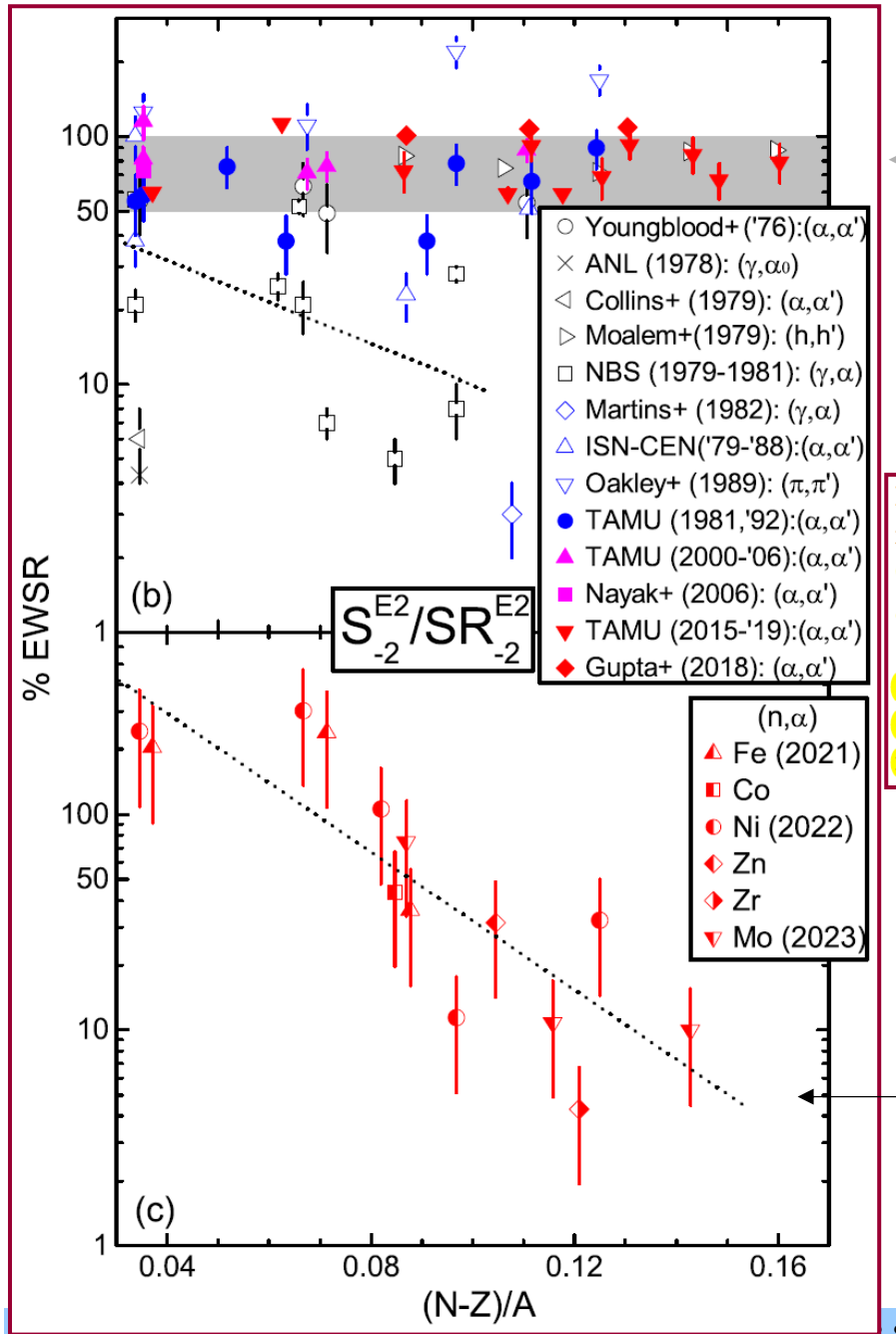

ISGQR: 50-100% of EWSR (±25%)

[M. N. Harakeh and A. van der Woude, *Giant Resonances Fundamental High-Frequency Modes of Nuclear Excitation* (Oxford University Press, New York, 2001) , p. 184]

Fig. 3. Comparison of EWSR fractions of ISGQR-*like* strength functions for neutron-induced α-emission on target nuclei with $54 \leq A \leq 98$ (Table 1), and ISGQR strength functions measured by inelastic scattering of ^{3}He and α-particles, and (γ,α) reaction [9,26,31,36–53], vs. (a) mass number A and (b,c) the $(N-Z)/A$ asymmetry parameter. There are included (b) the band of systematic values between 50–100% for the latter data, and a linear fit (dotted line) of the (γ,α) measurements [39,40,42], and (c) a linear fit (dotted line) of the neutron-induced α-emission results.

'effective' Q-value effect

[(n,p), (n,α) reactions *"isotope effect"*:

D.G. Gardner: NP **29**, 73 (1962);

H.L. Pai et al., NPA **164**, 526 (1971): $Q'_{(a,b)}=Q_{(a,b)}+\Delta_A-\Delta_B$

N.I. Molla, S.M. Qaim: NPA **283**, 269 (1977)**]**

4. (n,α) ISGQR / EWSR systematics vs. G_{syst}(2001) and Lorentzian ISGQR (1/4)

[PLB **858** (2024) 139078 *Suppl. Material:* https://www.sciencedirect.com/science/article/pii/S0370269324006361#ec0010:
***The ISGQR systematics' widths** and **Lorentzian shapes** use within neutron-induced α-emission analysis*]

Table 1
The ISGQR energies [24] and the ISGQR-*like* peak cross sections given in this work (if not previously[a,b,c]) for neutron-induced α-emission, corresponding to ISGQR Gaussian distribution with either the average FWHM value of $(16.0\pm1.8)/A^{1/3}$ MeV [24] or its lower limit[d] $14.2/A^{1/3}$ MeV, the corresponding integrated yields and ISGQR strength functions S^{E2}_{-2} as well as their EWSR fractions SR^{E2}_{-2}.

Excited nucleus	E_0 [24] (MeV)	σ_0 (mb)	Γ (MeV)	$\int\sigma^{GQR}dE$ (mb MeV)	S^{E2}_{-2} (μb/MeV)	($\%\,SR^{E2}_{-2}$)
^{55}Fe	16.829	4	3.73[d]	15.9	56.1	144
^{57}Fe	16.630	6[a]	4.16	26.6	96.0	248
^{58}Fe	16.534	0.8	3.67[d]	3.12	11.4	29.7
^{60}Co	16.348	1	4.09	4.35	16.3	39.7
^{59}Ni	16.440	8[b]	3.65[d]	31.1	115	259
^{61}Ni	16.258	8[b]	4.07	34.6	131	299
^{62}Ni	16.170	2.6[b]	4.04	11.2	42.8	98.2
^{63}Ni	16.084	0.3[b]	4.02	1.28	5.0	11.5
^{65}Ni	15.918	0.8[b]	3.98	3.39	13.4	31.2
^{68}Zn	15.680	0.9	3.92	3.76	15.3	31.5
^{92}Zr	14.177	0.24	3.15[d]	0.804	4.0	5.1
^{93}Mo	14.126	3[c]	3.53	11.3	56.5	66.0
^{96}Mo	13.977	0.6[c]	3.10[d]	1.98	10.1	12.0
^{99}Mo	13.835	0.5	3.07[d]	1.63	8.5	10.2

[a]Ref. [13], with eventual minor changes due to slightly different ISGQR energies [24,27].
[b]Ref. [14], as above.
[c]Ref. [8], as above.

Table 2
The ISGQR energies and lower limit $14.2/A^{1/3}$ MeV of the average FWHM values [24], and the ISGQR-*like* peak cross sections given in this work (if not previously[a,b,c]) for neutron-induced α-emission and ISGQR Lorentzian distribution, the corresponding integrated yields and ISGQR strength functions S^{E2}_{-2} as well as their EWSR fractions SR^{E2}_{-2}.

Excited nucleus	E_0 [24] (MeV)	σ_0 (mb)	Γ (MeV)	$\int\sigma^{GQR}dE$ (mb MeV)	S^{E2}_{-2} (μb/MeV)	($\%\,SR^{E2}_{-2}$)
^{55}Fe	16.829	4	3.73	23.5	82.8	212
^{57}Fe	16.630	6[a]	3.71	34.8	126	325
^{58}Fe	16.534	0.8	3.67	4.61	16.9	43.9
^{60}Co	16.348	1	3.63	5.70	21.3	52.0
^{59}Ni	16.440	8[b]	3.65	45.8	170	383
^{61}Ni	16.258	8[b]	3.61	45.3	172	391
^{62}Ni	16.170	2.6[b]	3.59	14.7	56.0	129
^{63}Ni	16.084	0.3[b]	3.57	1.68	6.5	15.0
^{65}Ni	15.918	0.8[b]	3.53	4.44	17.5	40.8
^{68}Zn	15.680	0.9	3.48	4.92	20.0	41.2
^{92}Zr	14.177	0.24	3.15	1.19	5.9	7.6
^{93}Mo	14.126	3[c]	3.13	14.8	74.0	86.4
^{96}Mo	13.977	0.6[c]	3.10	2.92	15.0	17.7
^{99}Mo	13.835	0.5	3.07	2.41	12.6	15.0

[a]Ref. [13], with eventual minor changes due to slightly different ISGQR energies [24,27].

First of all, it should be noted that the ISGQR-*like* widths for five of the fourteen nuclei in Table 1 (^{57}Fe, ^{61,63,65}Ni, ^{68}Zn) agree within 4% with the average value $\Gamma=(16.0\pm1.8)/A^{1/3}$ MeV [24]. Additionally, the widths and are even higher by 9%–13% for three other nuclei (^{60}Co, ^{62}Ni, ^{93}Mo) in this table, but roughly lower for the remaining ones (^{55,58}Fe, ^{59}Ni, ^{92}Zr, ^{96,99}Mo). Despite

[24] M. N. Harakeh and A. van der Woude, *Giant Resonances Fundamental High-Frequency Modes of Nuclear Excitation* (Oxford University Press, New York, 2001).

4. (n,α) ISGQR / EWSR systematics vs. $G_{syst}(2001)$ and Lorentzian ISGQR (2/4)

[PLB **858** (2024) 139078 *Suppl. Material:* https://www.sciencedirect.com/science/article/pii/S0370269324006361#ec0010 :
***The ISGQR systematics' widths** and **Lorentzian shapes** use within neutron-induced α-emission analysis*]

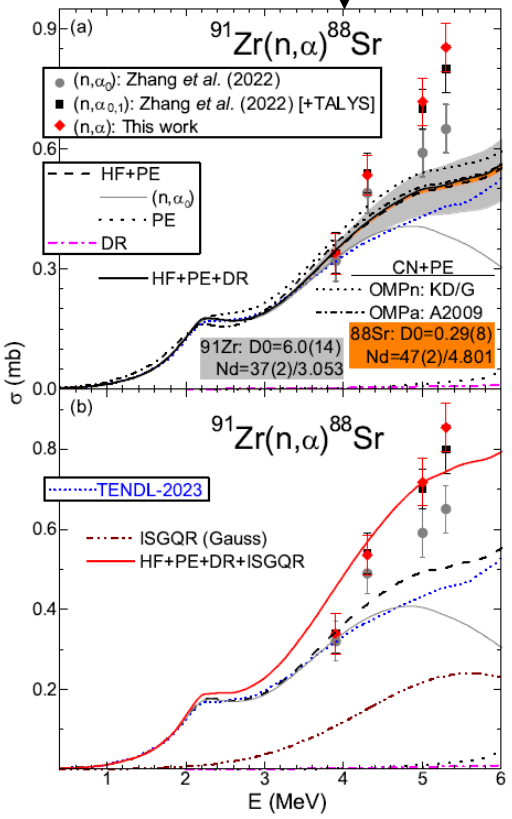

Fig. 1. (Color online) Comparison of cross sections measured [1] (symbols with error-bars) with model calculations (solid and dashed curves). Panels show measured data for ^{91}Zr$(n,\alpha_0)^{88}$Sr reaction (circles) and deduced for $(n,\alpha_{0,1})$ reaction [1] (squares) and (n,α) reaction (diamonds), and compare them to calculated values for (n,α) reaction DR (dash-dotted), PE (dotted), and HF+PE (dashed) components. In particular, we show (a) HF+PE+DR sum (solid), HF+PE uncertainty bands related to the error bars of fitted N_d and D_0^{exp} by level densities of target ^{91}Zr (gray) and residual nucleus ^{88}Sr (orange), and HF+PE results using other OMPs for α-particles [22] (short-dash-dotted) or neutrons [23] (short-dashed), and (b) the ISGQR component corresponding to a Gaussian distribution for the extra-yield beyond the DR+PE+CN calculated cross sections (dash-dot-dotted), and HF+PE+DR+ISGQR sum (solid).

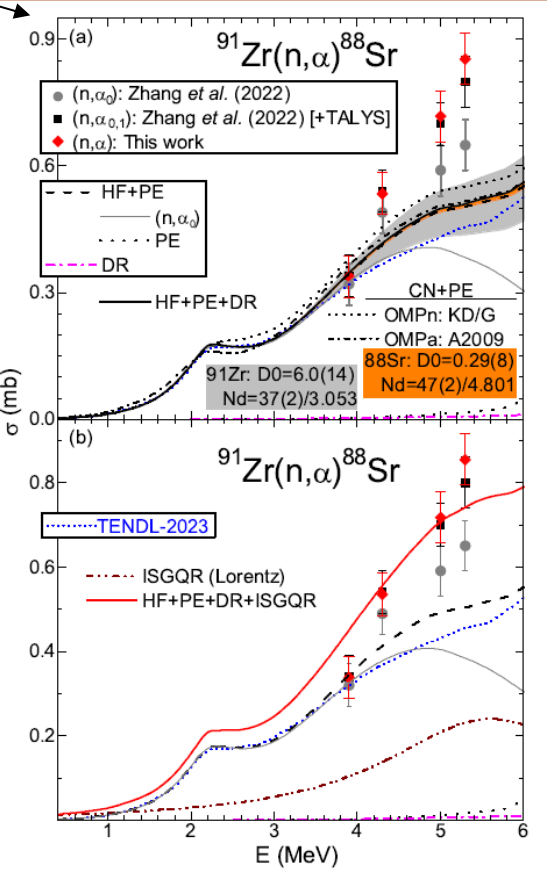

Fig. 4. (Color online) As Fig. 1 but for assumption of a Lorentzian distribution for the extra-yield beyond the DR+PE+CN calculated cross sections (dash-dot-dotted).

4. (n,α) ISGQR / EWSR systematics vs. G_{syst}(2001) and Lorentzian ISGQR (3/4)

[PLB **858** (2024) 139078 *Suppl. Material:* https://www.sciencedirect.com/science/article/pii/S0370269324006361#ec0010:
***The ISGQR systematics' widths** and **Lorentzian shapes** use within neutron-induced α-emission analysis*]

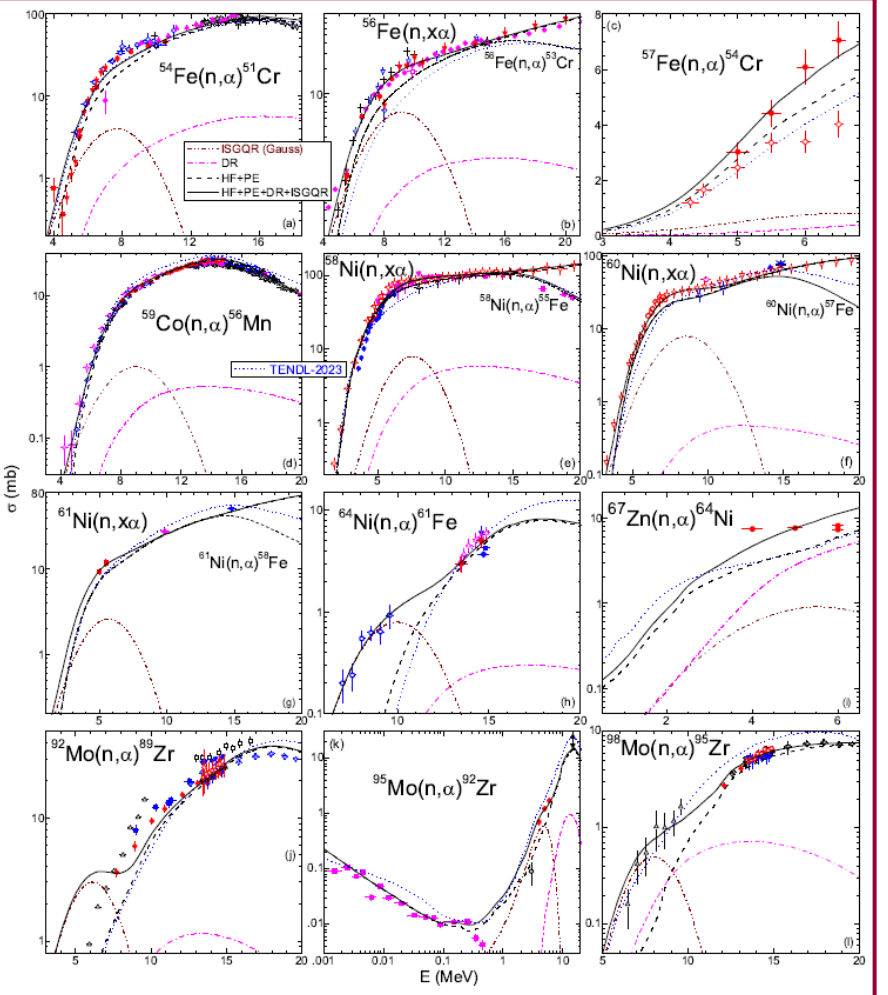

Fig. 2. (Color online) Comparison of measured [15] and calculated neutron-induced α-emission cross sections (solid curves) for ^{54,56,57}Fe, ^{59}Co, ^{58,60,61,62,64}Ni, ^{67}Zn, and ^{92,95,98}Mo target nuclei, including the ISGQR (dash-dot-dotted), DR (dash-dotted), and HF+PE (dashed) components, and HF+PE uncertainty bands for the residual-nuclei level densities [8,13,14]. The ISGQR components correspond to a Gaussian distribution (Table 1) for the extra-yield beyond the DR+PE+CN calculated cross sections.

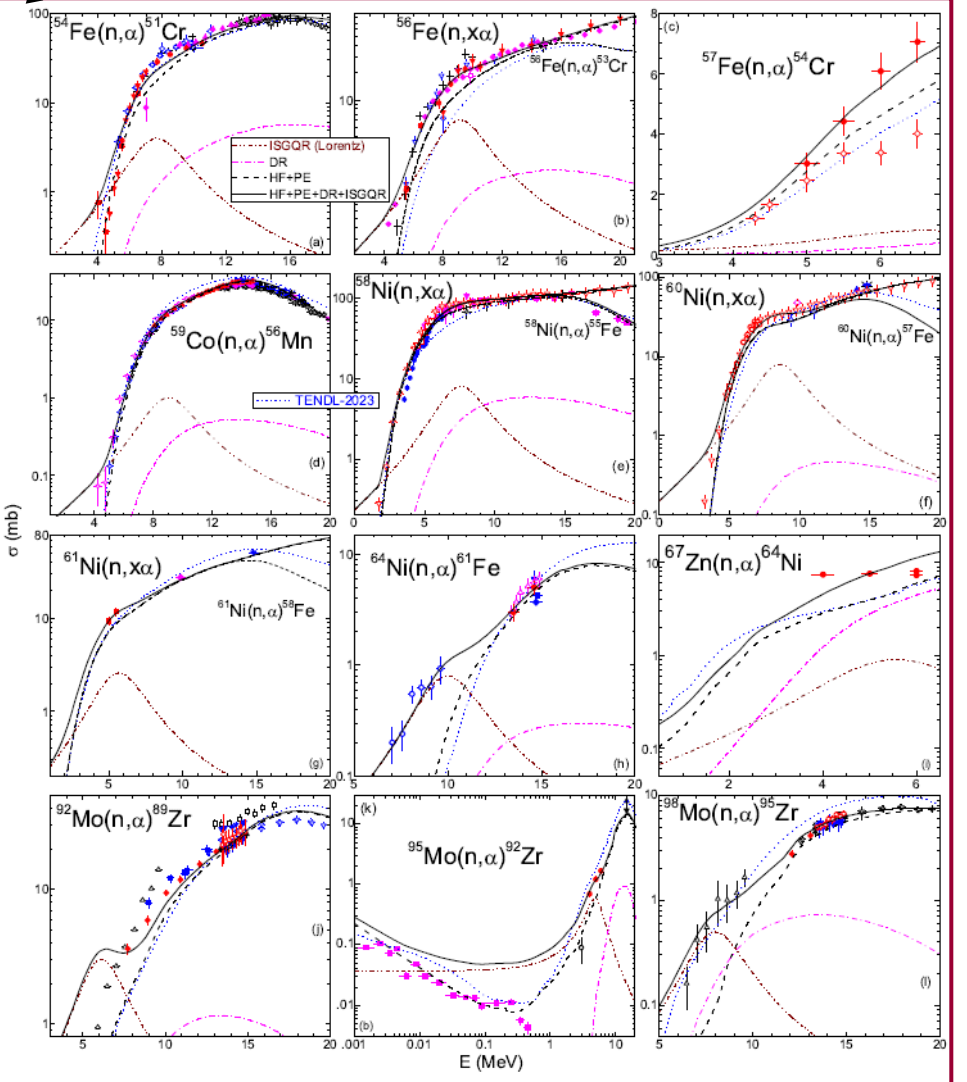

Fig. 5. (Color online) As Fig. 2 but for ISGQR components corresponding to the assumption of a Lorentzian distribution (Table 2) for the extra-yield beyond the DR+PE+CN calculated cross sections.

4. (n,α) ISGQR / EWSR systematics vs. $G_{syst}(2001)$ and Lorentzian ISGQR (4/4)

[PLB **858** (2024) 139078 *Suppl. Material:* https://www.sciencedirect.com/science/article/pii/S0370269324006361#ec0010:
***The ISGQR systematics' widths** and **Lorentzian shapes** use within neutron-induced α-emission analysis*]

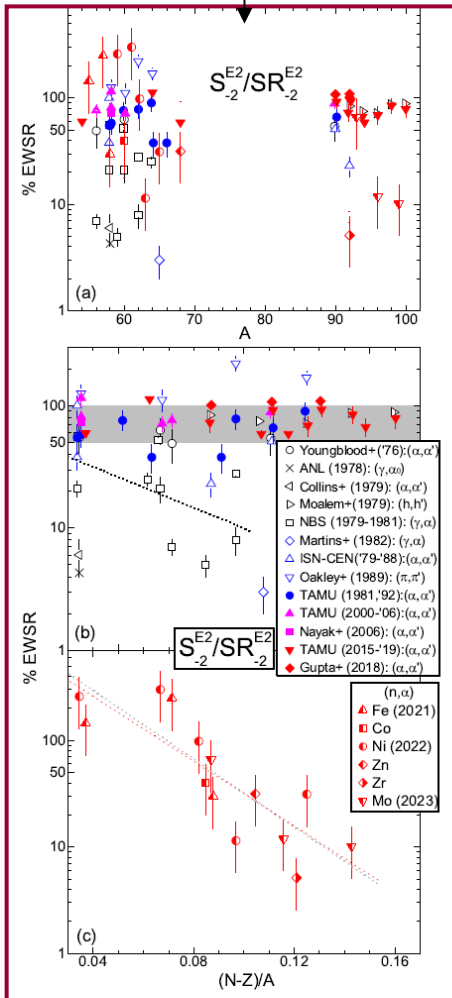

Fig. 3. (Color online) Comparison of EWSR fractions of ISGQR strength functions for neutron-induced α-emission on target nuclei with $54 \leq A \leq 98$ (Table 1), and ISGQR strength functions measured by inelastic scattering of ^{3}He and α-particles, and (γ,α) reaction [9,26,31,36–53], vs. (a) mass number A and (b,c) the $(N-Z)/A$ asymmetry parameter. There are included (b) the band of systematic values between 50–100% for the latter data, and a linear fit (dotted line) of the (γ,α) measurements [39,40,42], and (c) a linear fit (dotted line) of the neutron-induced α-emission results.

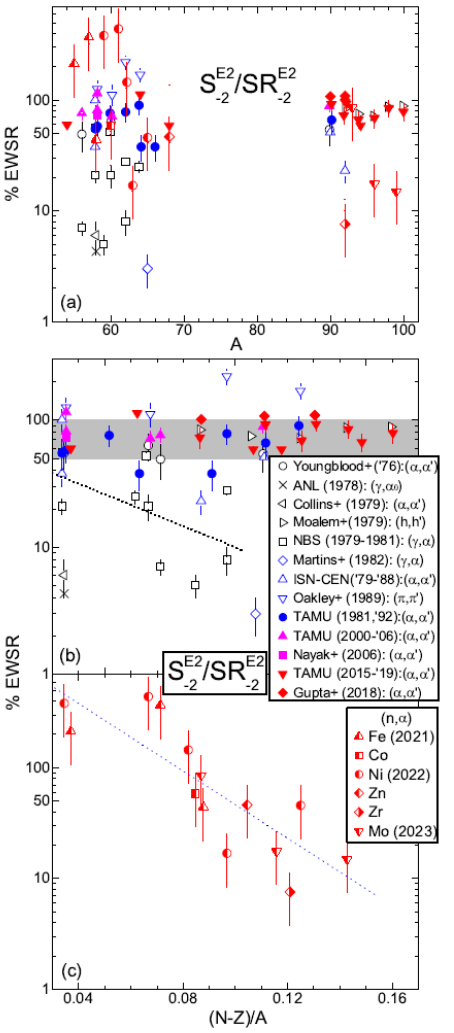

Fig. 6. (Color online) As Fig. 3 but for ISGQR components corresponding to the assumption of a Lorentzian distribution (Table 2) for the extra-yield beyond the DR+PE+CN calculated cross sections.

4. Conclusions

Latest results concerning alpha-particle emission (confirmed):

- **α-OMP A+(2014): suitable description [NO fit/normalization] + DI + (ISGQR)**
- **NO emitted α-particle OMP parameters**
- **(n,α) / (p,α) reaction systematical analysis**
- **ISGQR EWSR systematics: 50-100% [(α,α')] vs. 100-10% [(x,α)], x=γ,n**
- **Further, next to** https://conferences.iaea.org/event/368/contributions/31753/ poster at Compound Nuclear Reactions and Related Topics (CNR*24), July 8-12, 2024, Vienna, IAEA
  - Possible microscopic path: - H. Sasaki *et al.* (LANL), CNR*24, 31760
    - P. Stevenson (Univ. Surrey), CNR*24, 31769
  - Preliminary new experimental data (Peking Univ., Beijing): ^{64,66,67}Zn(n,α)

Availability for (n,x), (p,x) activation evaluation

[Fe, Co, Cu, Ni, Zn, Zr, Nb, Mo (2021-2023)
- available data analysis/description
- additional calculations on request]

Thank you for your attention !

PNIII-P4-PCE-2021-0642

WPBB-S.05.02-T007-D005

JEFF NDW, Session Fusion, Nov. 2024, EFFDOC-1546
(EUROfusion WPBB-S.05.02-T007 Monitoring meeting)
[https://www.oecd-nea.org/dbdata/nds_effdoc/effdoc-1546.pdf]

Progress Report on deuteron-induced reaction analysis

[EUROfusion WPBB-S.05.02-T007-D005: Advanced analysis of isomeric cross sections of deuteron-induced reactions on A=90-100 nuclei]

Marilena Avrigeanu and Vlad Avrigeanu

Horia Hulubei National Institute for Physics & Nuclear Engineering, (IFIN-HH), Bucharest, Romania

Content

1. WPBB-S.05.02-T007-D005 Obj./Del. [https://ims.euro-fusion.org]

Task Specification (TS)

TS Title:	Nuclear Data Evaluations - 2024		
TS Ref. Nr.:	BB-S.05.02-T007	Task coordinator:	Dieter Leichtle
Status:	In review	Date:	14-Feb-2024

D005: Technical Specification: Advanced analysis of isomeric cross sections of deuteron-induced reactions on A=90-100 nuclei (IAP)

A suitable account of the measured ground and isomeric state excitation functions of deuteron-induced reactions on Zr and Mo stable isotopes and natural elements has been obtained within actual state-of-art TALYS calculations by amending the nuclear-level density (NLD) spin distribution cut-off parameter by a factor of 0.25 [EUROFUSION WPBB-PR(24) 36171]. Actually these results are in line with the most recent compilation of isomeric ratios of light particle induced reactions [At. Data Nucl.Data Tables **153**, 101583 (2023)]. On the other hand, a large amount of measured isomeric cross sections of reactions induced by deuterons on Nb [Phys. Rev. C **88**, 014612 (2013)] as well as neutrons on Mo [Phys. Rev. C **71**, 044617(2005)] was already well described using no spin cut-off adjustment but an advanced particle-hole state density [Comp. Phys. Comm. **112**, 191 (1998)] including a PE spin cut-off [Nucl. Sci. Eng. **92**, 440 (1986)]. These results agree with the previous conclusion that reduced values of the spin cut-off parameter, obtained from isomeric cross-section analysis, were artificial and resulted from the use of an improper pre-equilibrium (PE) spin distribution, namely the compound-nucleus (CN) spin distribution [Phys. Rev. C **80**, 044612 (2009)]. Therefore, an advanced analysis of isomeric cross sections of deuteron-induced reactions on A=90-100 nuclei is aimed in this work, next to the proper account of the contributions of all involved reaction mechanisms as the breakup, stripping, pick-up, PE and CN processes, with the results provided in the TALYS code format. At the same time it will be taken the advantage of becoming available similar data just measured at Ganil on Mo up to 40 MeV.

PM: 3 PM (IAP)

ID	Title	Start Date	End Date	RU	Del. Owner	AWP2024 PM 50% standard
BB-S.05.02-T007 - D005	Advanced analysis of isomeric cross sections of deuteron-induced reactions on A=90-100 nuclei	01-Jan-24	31-Dec-24	IAP	Marilena Avrigeanu	3.000

Dedicated projects to IFMIF and ITER: EURATOM, F4E, EUROfusion

PHYSICAL REVIEW C **79**, 044610 (2009)

Low and medium energy deuteron-induced reactions on ^{27}Al

PHYSICAL REVIEW C **84**, 014605 (2011)

Low and medium energy deuteron-induced reactions on ^{63,65}Cu nuclei

PHYSICAL REVIEW C **88**, 014612 (2013)

Low-energy deuteron-induced reactions on ^{93}Nb

PHYSICAL REVIEW C **89**, 044613 (2014)

Low energy deuteron-induced reactions on Fe isotopes

PHYSICAL REVIEW C **94**, 014606 (2016)

Deuteron-induced reactions on Ni

PHYSICAL RE… (2018)

Consistent acco… reactions on ^{nat}Cr up to 60 MeV

PHYSICAL REVIEW C **101**, 024605 (2020)

Deuteron-induced reactions on manganese at low energies

PHYSICAL REVIEW C **104**, 044615 (2021)

Deuteron-induced reactions on ^{nat}Zr up to 60 MeV

Journal of Fusion Energy (2024) **43**:15

Modeling of Deuteron-Induced Reactions on Molybdenum at Low Energies

EURATOM

d+Al,
d+Cu,
d+Nb

GRT … for … Energy (F4E)

d+Fe
d+Ni

EUROfusion

d+Cr
d+Mn

SPIRAL 2

d+Zr

EUROfusion

d+Mo

Priority list of IFMIF-DONES candidate materials

Deuteron-nucleus interaction analysis

Motivation: Nuclear Data Needs: ITER, IFMIF, SPIRAL2, SARAF, Medical Installations

DEUTERONS BEAM

Associated Research Projects: New data & Updated theory

FENDL, EURATOM, F4E, EUROfusion

- **Breakup – in TALYS-1.96, option breakupmodel 2:** M. Avrigeanu *et al.*, **Eur. Phys. J. A (2022) 58:3**

  BREAKUP [M. Avrigeanu, V. Avrigeanu]

  - parametrization of total BU protons & elastic-breakup c.s.:

  - inelastic breakup enhancement brought by **breakup-nucleons** reactions

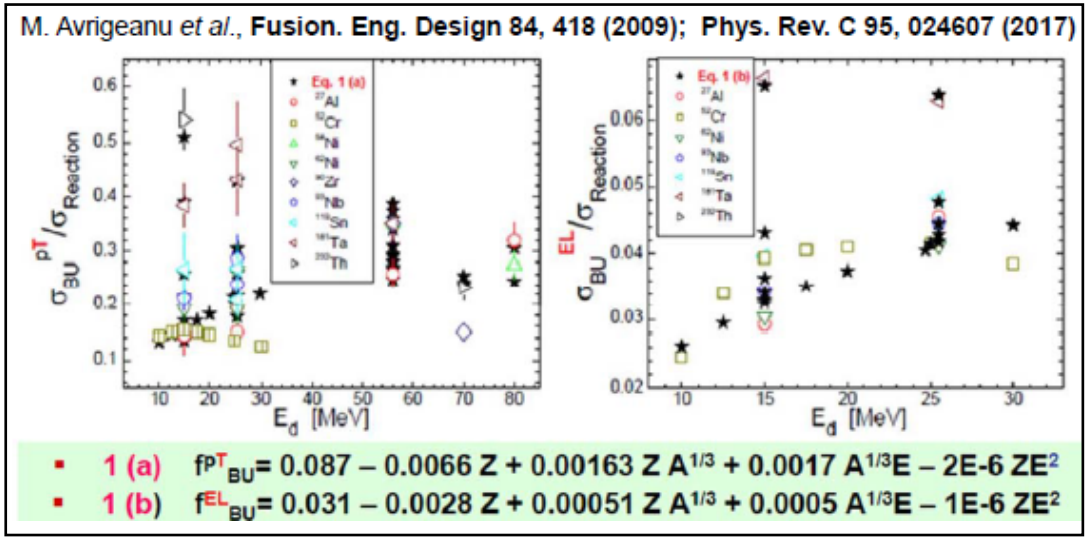

- **Direct reactions**

  FRESCO (Version **FRES 2.9**) [I.J. Thompson]

  - stripping & pick-up, DWBA : (d,p), (d,n), (^{3}He,d), (d,t), (d,α), (d,^{3}He)

- **Composite system equilibration for both deuteron and breakup-nucleon reactions**

  STAPRE-H95 [V. Avrigeanu, M. Avrigeanu] (updated)

  - OMP:SCAT2000; preequilibrium (PE): **GDH / EXCITON;** evaporation: **Hauser-Feshbach**

  TALYS - 1.0 - 1.97 [A. Koning, S. Hilaire, S. Goriely]

  - OMP:ECIS'97; breakup, preequilibrium (PE): **MSD / EXCITON;** evaporation: **Hauser-Feshbach**

TALYS-2.0

Simulation of nuclear reactions

Arjan Koning, Stephane Hilaire, Stephane Goriely

Fermi gas spin distribution

$$R_F(E_x,J)=\frac{2J+1}{2\sigma^2}\exp\left[-\frac{(J+\frac{1}{2})^2}{2\sigma^2}\right]$$

$$\sigma^2=\sigma_{\parallel}^2=\sigma_F^2(E_x)=I_0\frac{a}{\tilde{a}}t, \qquad (8.23)$$

with $\tilde{a}$ from Eq. (8.13) and

$$I_0=\frac{\frac{2}{5}m_0R^2A}{(\hbar c)^2}, \qquad \text{moment of inertia of the nucleus } I_0 \qquad (8.24)$$

thermodynamic temperature t,

$$t=\sqrt{\frac{U}{a}}. \qquad (8.22)$$

$$\sigma_F^2(E_x)=0.01389\frac{A^{5/3}}{\tilde{a}}\sqrt{aU}. \qquad (8.25)$$

On average, the $\sqrt{aU}/\tilde{a}$ has the same energy- and mass-dependent behaviour as the temperature $\sqrt{U/a}$. The differences occur in the regions with large shell effects. Eq. (8.25) can be altered by means of **Rspincut** $= I/I_0$:

Range

0. ≤ Rspincut ≤ 10.

Default

Rspincut 1.

preeqspin

Flag to use the pre-equilibrium or compound nucleus spin distribution for the pre-equilibrium population of the residual nuclides. For backward-compatibility with earlier versions of TALYS, the following options are now possible:

Examples

preeqspin n or **preeqspin 1**: the pre-equilibrium spin distribution is made equal to the relative spin-dependent population after compound nucleus emission
preeqspin 2: the spin distribution from total level densities is adopted
preeqspin y or **preeqspin 3**: the pre-equilibrium spin distribution is based on particle-hole state densities

Range

y or **n**, or **1** ≤ **preeqspin** ≤ **3**.

Default

preeqspin n

12.3 Pre-equilibrium spin distribution

The function $R_n(J)$ represents the spin distribution of the states in the continuum. It is given by

$$R_n(J) = \frac{2J+1}{\pi^{1/2} n^{3/2} \sigma^3} \exp\left[-\frac{(J+\frac{1}{2})^2}{n\sigma^2}\right], \quad (12.59)$$

The used expression for the spin cut-off parameter σ is that by Gruppelaar et al. [108],

$$\sigma^2 = 0.24 n A^{\frac{1}{3}}. \quad (12.61)$$

Options 12.3.1 With **preeqspin y** (p. 596) Eq. (12.61) is invoked. Another option is the more a microsopic-based QRPA expression from Dupuis et al. [109].

rspincutpreeq

$$\sigma_n^2 = 0.04 n A^{2/3}$$

```
- December 7, 2022

Added pre-equilibrium spin distribution model 'preeqspin 4' from Marc
Dupuis inferred from JLM/QRPA calculations. Also added keyword
'Rspincutpreeq' to adjust pre-equilibrium spin cutoff parameter.
```

Effects of various options for level density spin distribution on d + Mo (d,xn)

projectile d
element Mo
mass 0
energy energies
popeps 1.e-12
partable y
#
bins 100
breakupmodel 2
deuteronomp 2
#
Preeqspin **1/y/4**
Rspincut **1.**; **0.5**; **0.25**
#
filetotal y

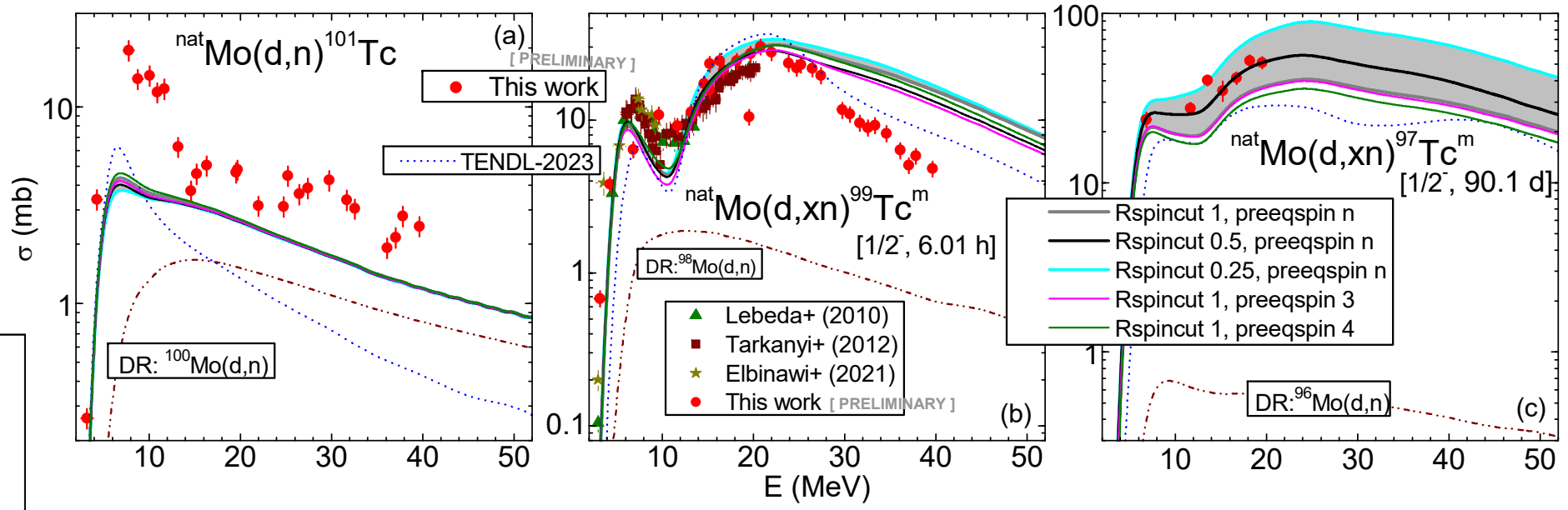

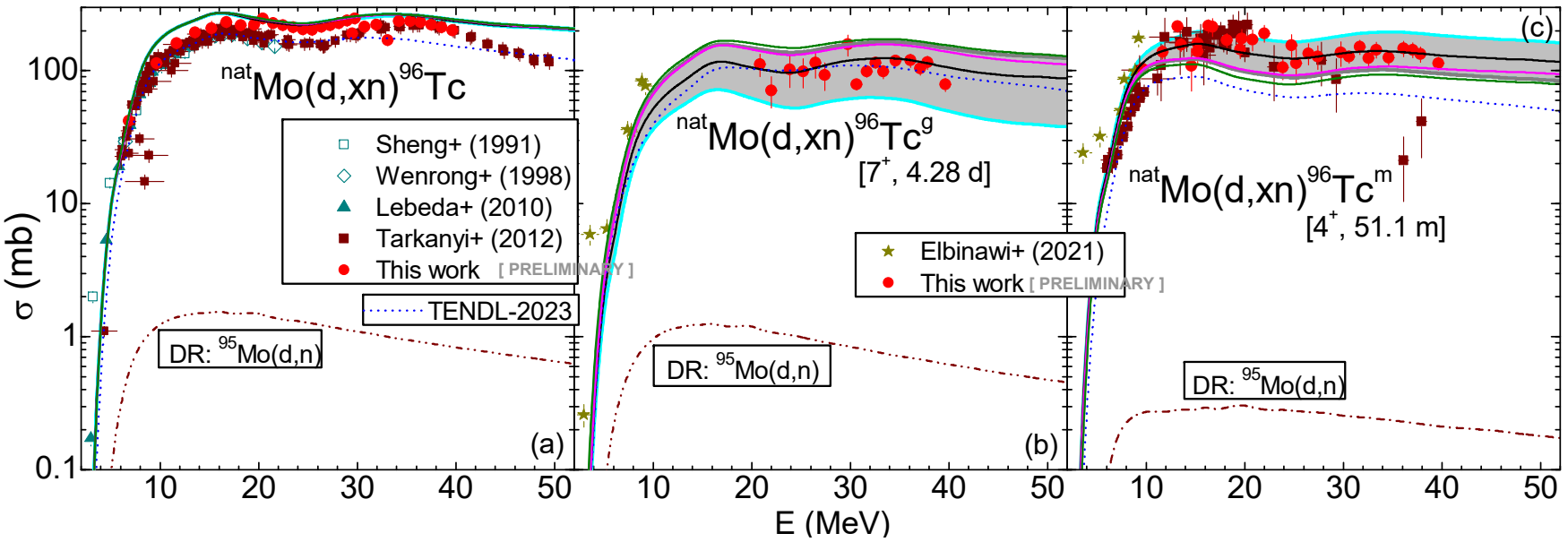

***decreasing I/I_0 ratio, Rspincut, or Rspincutpreeq (preeqspin 4), increases low spin isomeric states population**

Effects of various options for level density spin distribution on d + Mo (d,xn)-2

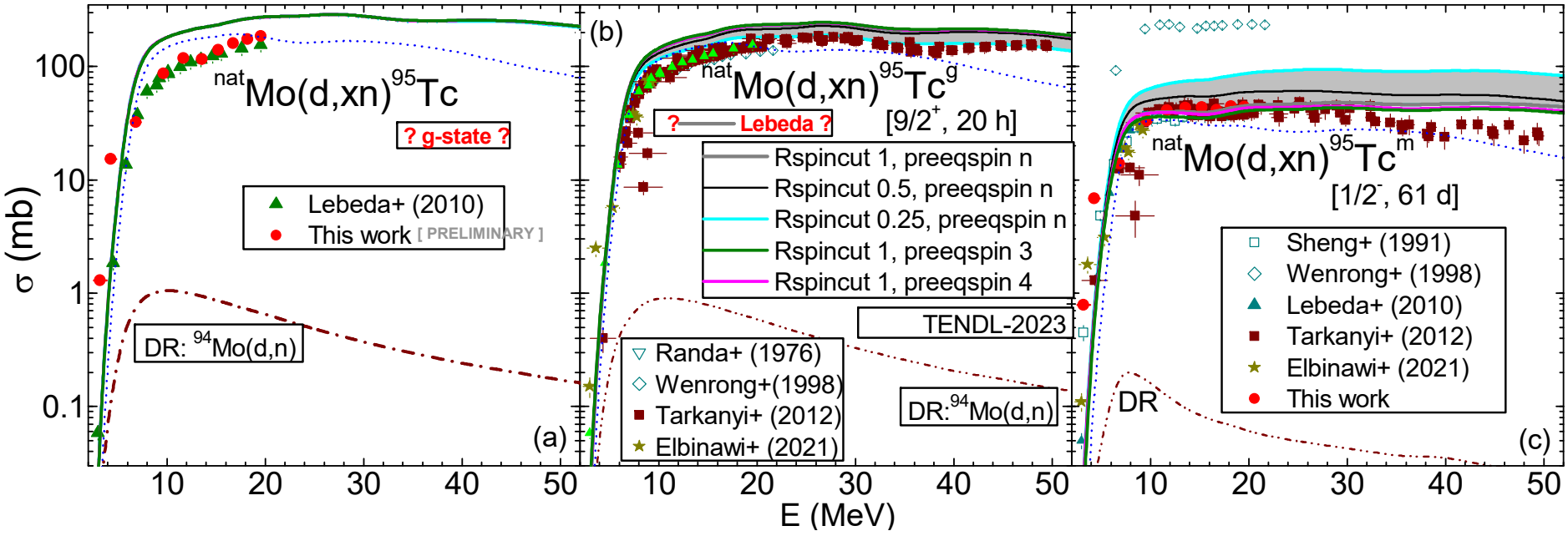


```
projectile d
element    Mo
mass       0
energy     energies
popeps 1.e-12
partable y
#
bins 100
breakupmodel 2
deuteronomp 2
#
Preeqspin 1/y/4
Rspincut 1.; 0.5; 0.25
#
filetotal y
```

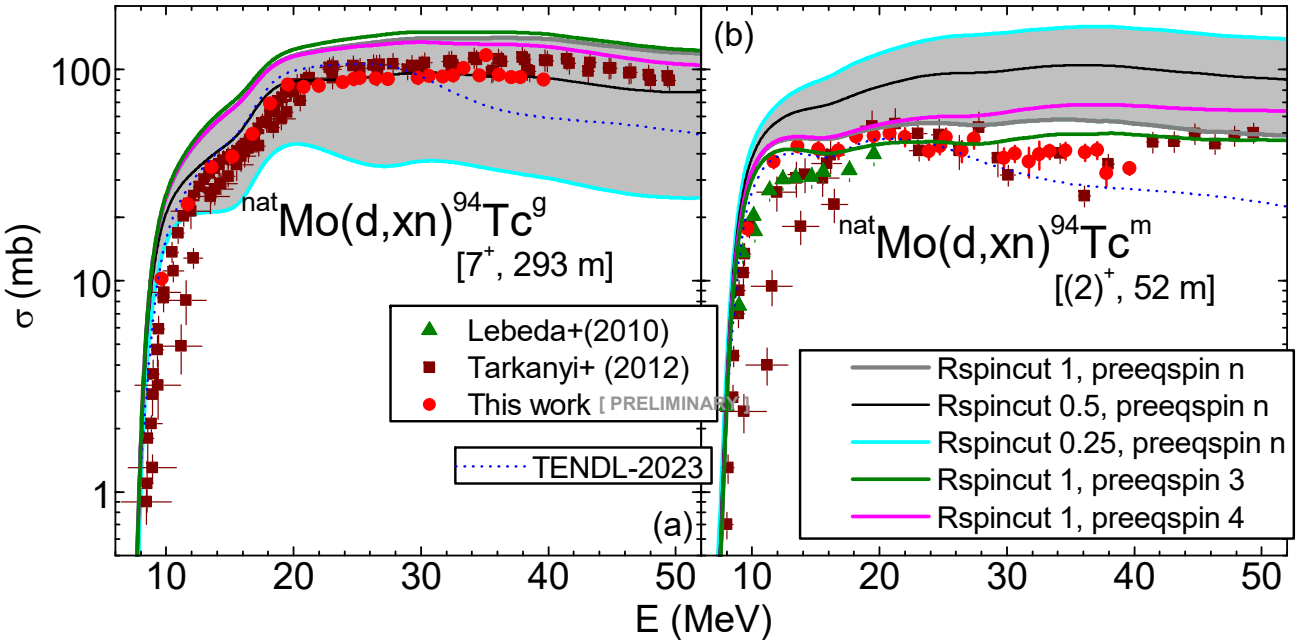

Effects of various options for level density spin distribution on d + Mo (d,xn)-3

```
projectile d
element    Mo
mass       0
energy     energies
popeps 1.e-12
partable y
#
bins 100
breakupmodel 2
deuteronomp 2
#
Preeqspin 1/y/4
Rspincut 1.; 0.5; 0.25
#
filetotal y
```

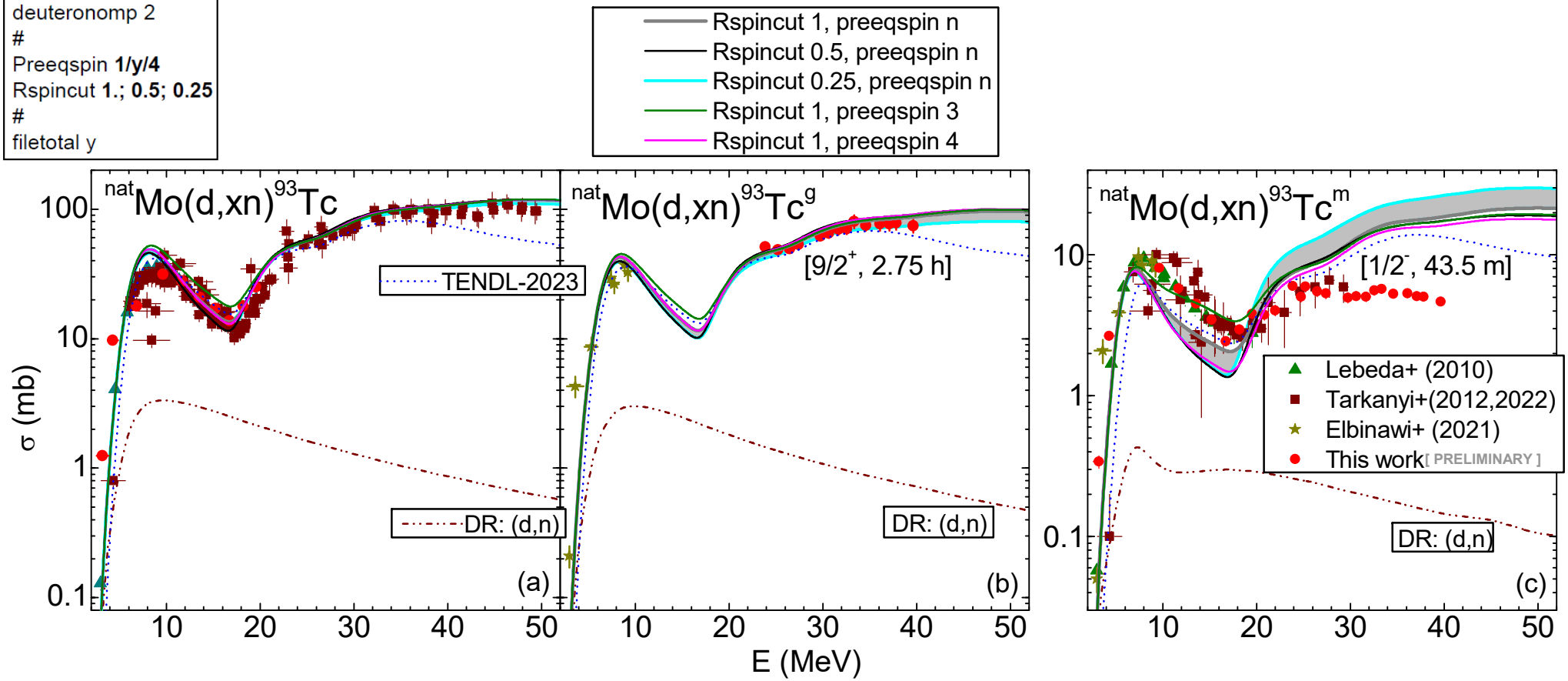

Effects of various options for level density spin distribution on d + Mo (d,xnp)

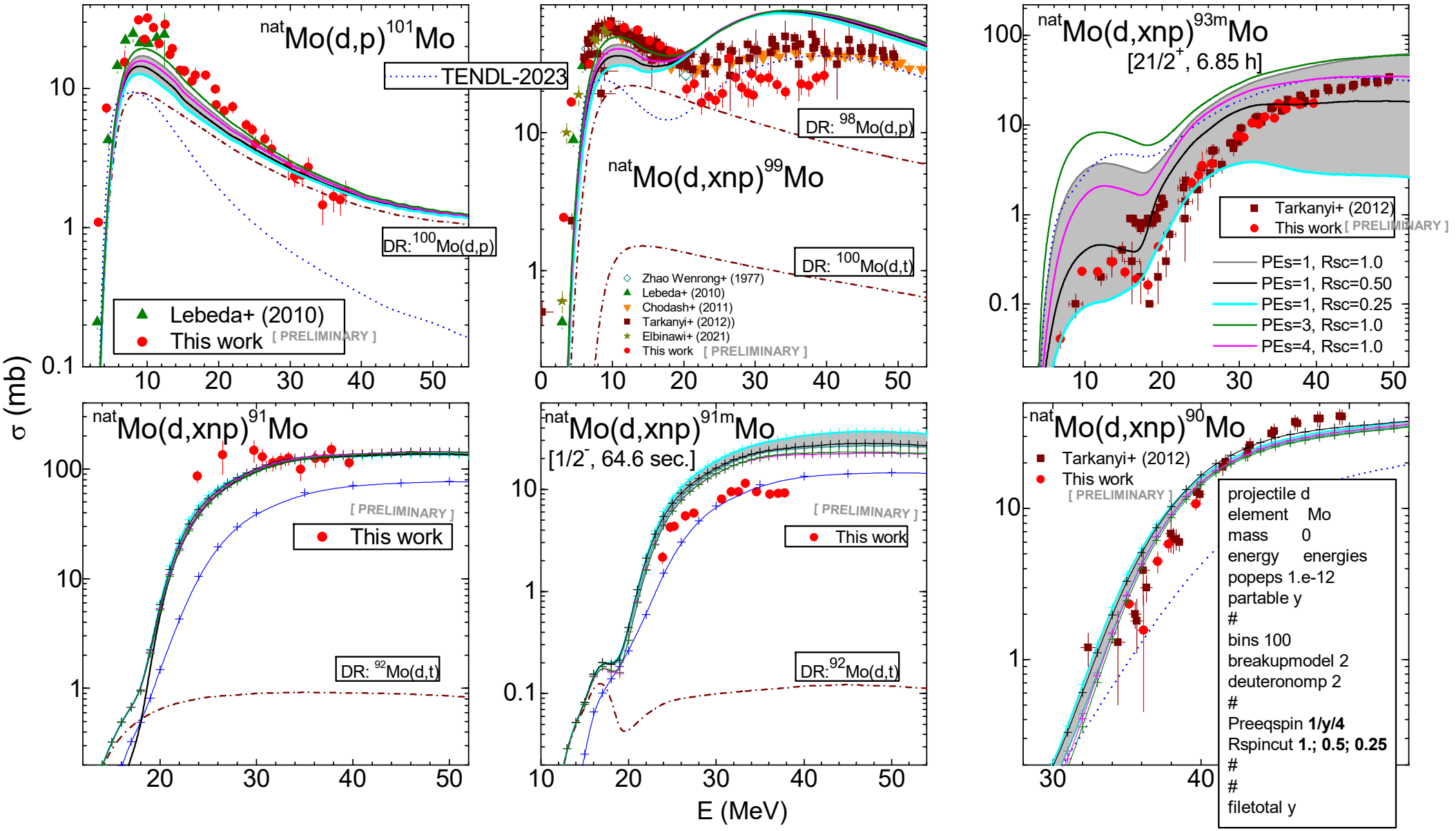

Effects of various options for level density spin distribution on d + Mo (d,xn2p)

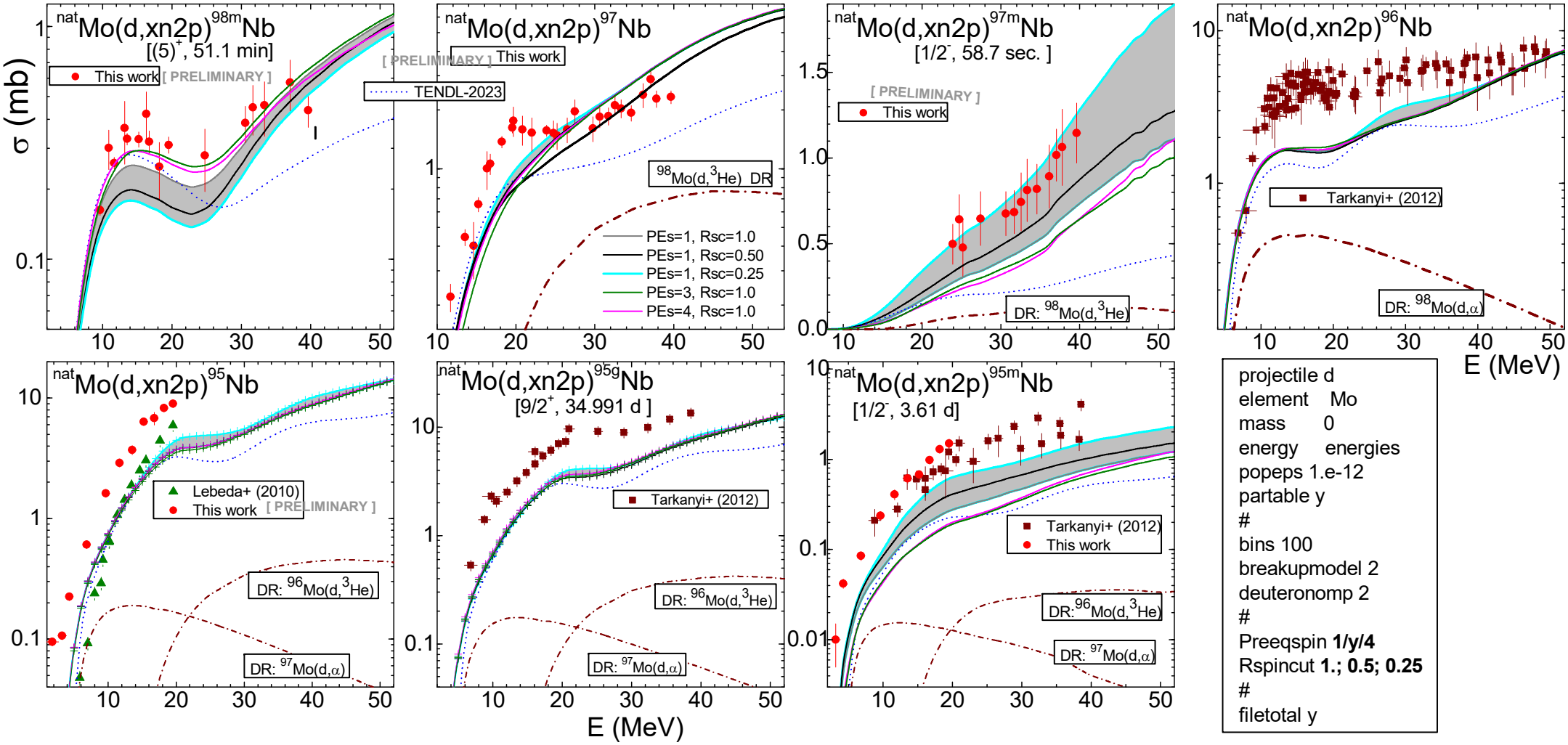


```
projectile d
element    Mo
mass       0
energy     energies
popeps 1.e-12
partable y
#
bins 100
breakupmodel 2
deuteronomp 2
#
Preeqspin 1/y/4
Rspincut 1.; 0.5; 0.25
#
filetotal y
```

Effects of various options for level density spin distribution on d + Mo (d,xn3p)

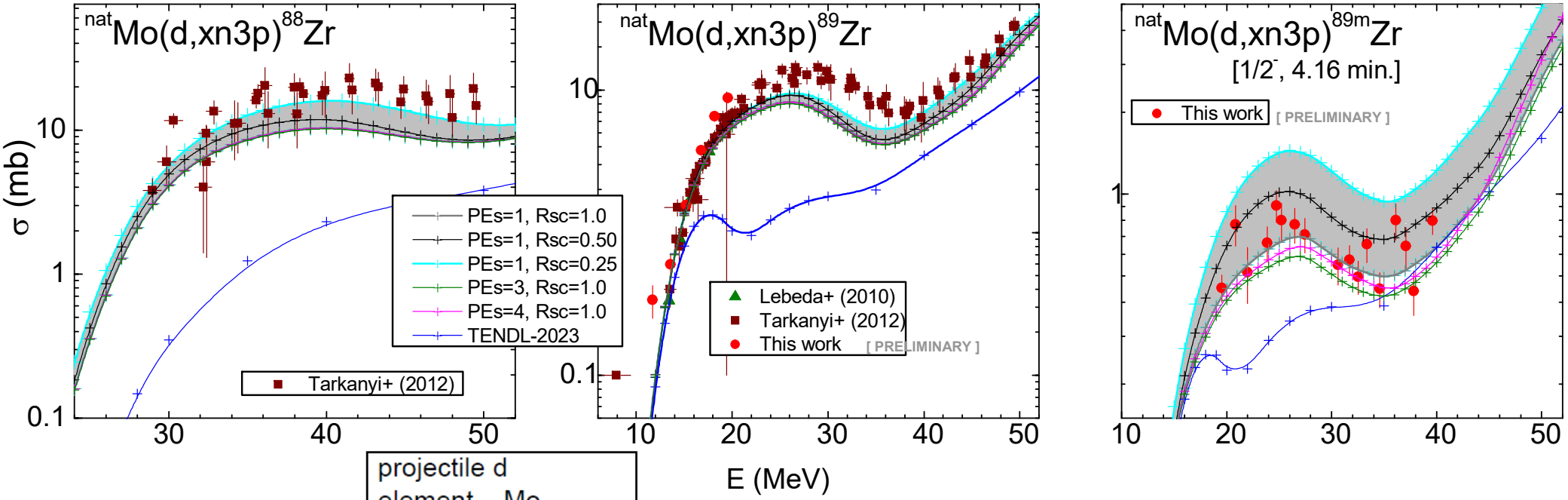


```
projectile d
element    Mo
mass       0
energy     energies
popeps 1.e-12
partable y
#
bins 100
breakupmodel 2
deuteronomp 2
#
Preeqspin 1/y/4
Rspincut 1.; 0.5; 0.25
#
filetotal y
```

Effects of various options for level density spin distribution on d + Zr (d,xn)

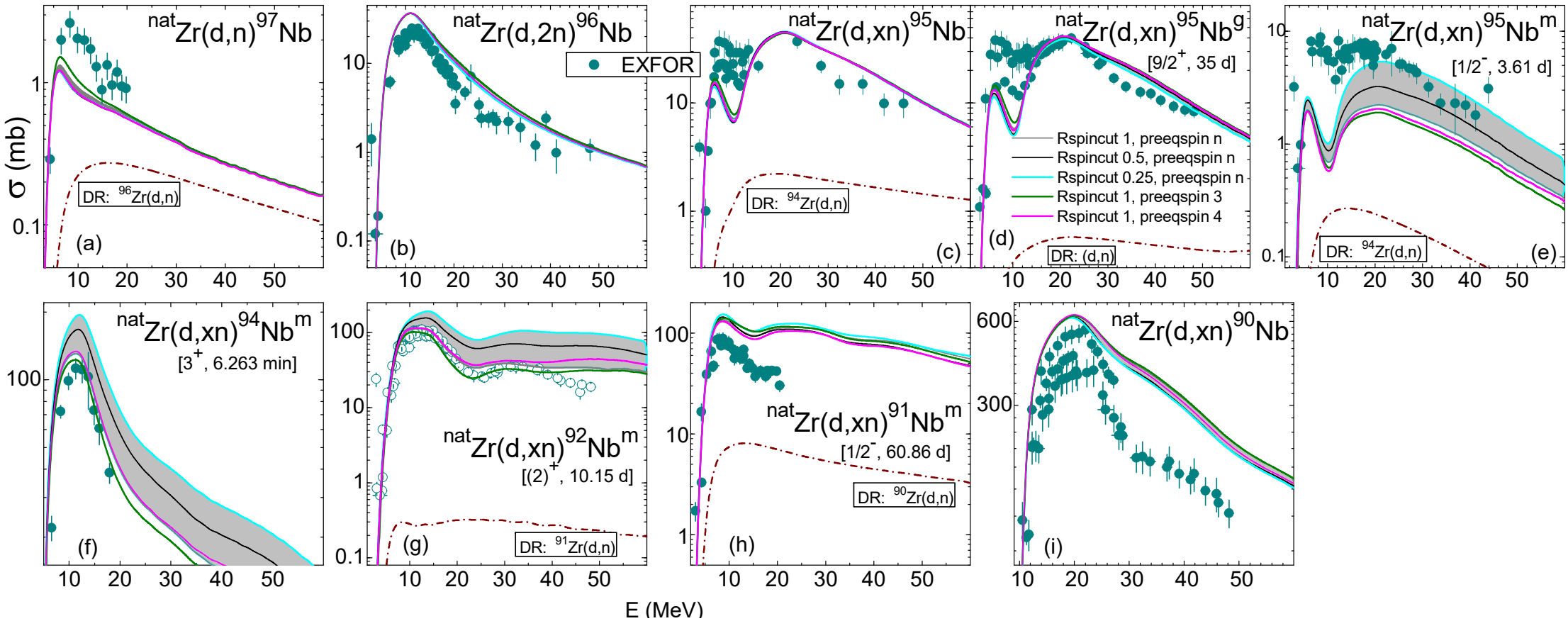

Effects of various options for level density spin distribution on d + Zr (d,xn2p)

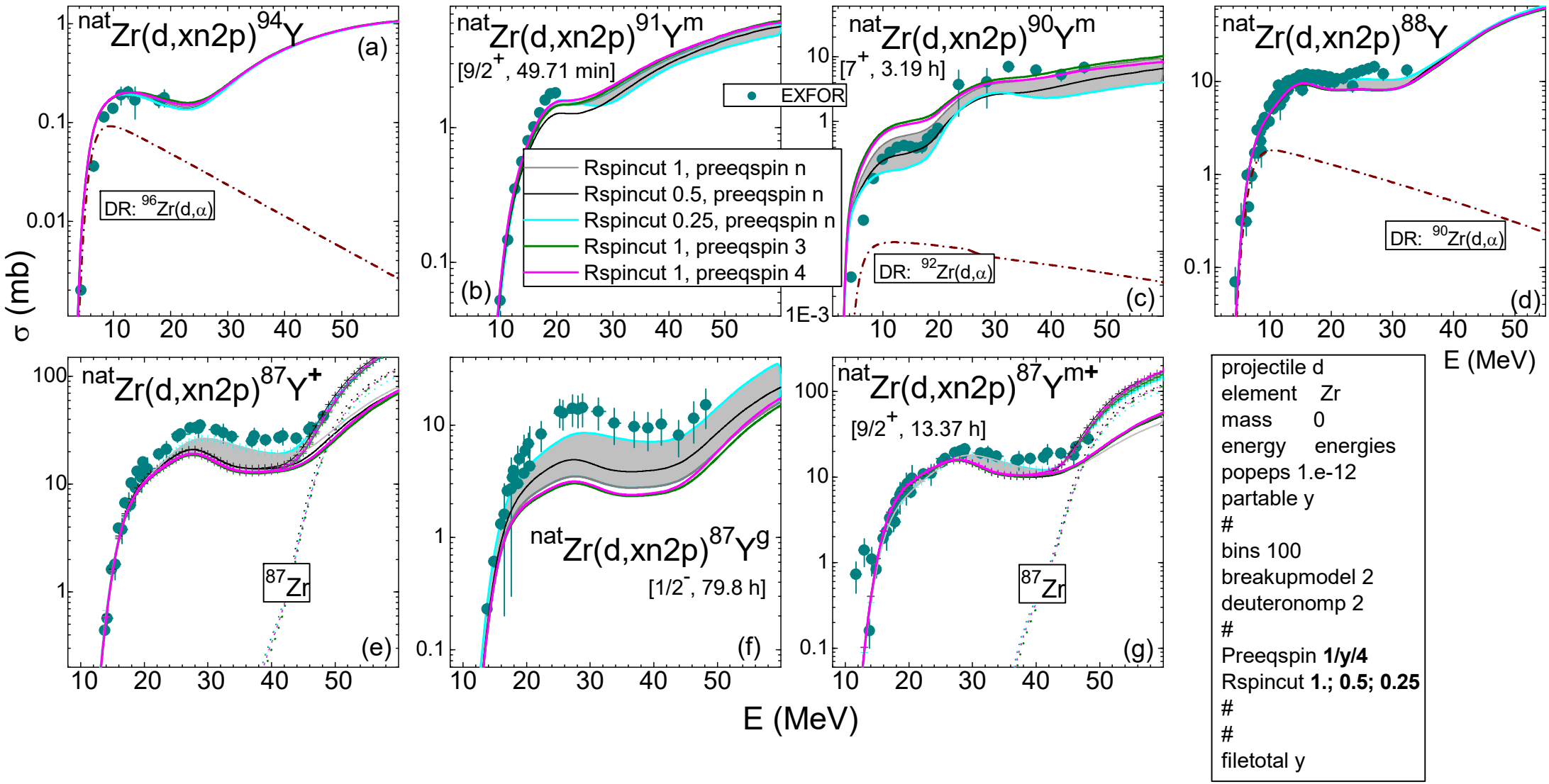


```
projectile d
element   Zr
mass      0
energy    energies
popeps 1.e-12
partable y
#
bins 100
breakupmodel 2
deuteronomp 2
#
Preeqspin 1/y/4
Rspincut 1.; 0.5; 0.25
#
#
filetotal y
```

Effects of various options for level density spin distribution on d + Nb

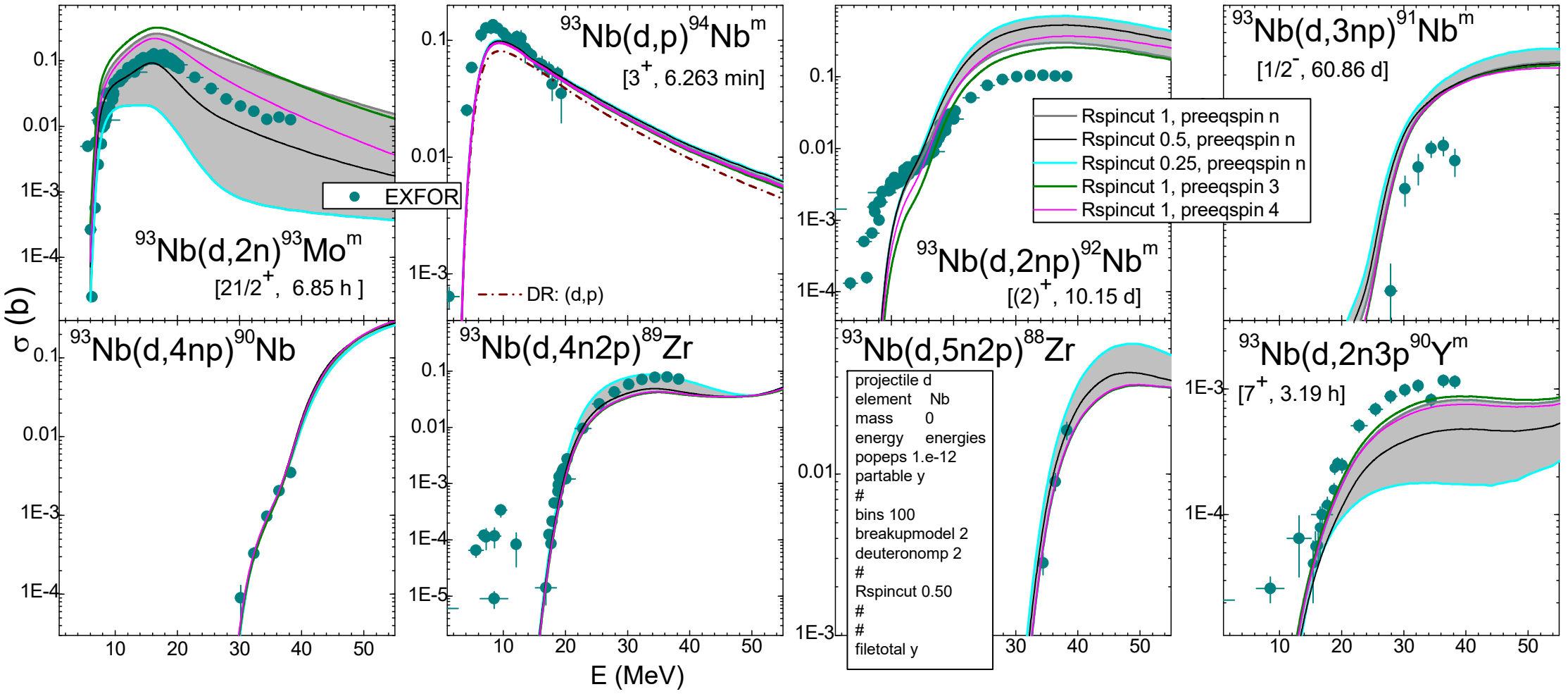

CONCLUSIONS

Thank you!

Effects of various options for specific level density spin distribution:

- **preeqspin 1 (def)**
  - ✓ **Rspincut 1. (def)**
  - ✓ **Rspincut 0.50**
  - ✓ **Rspincut 0.25**
- **preeqspin 3**
  - ✓ **Rspincut 1.; Rspincutpreeq 1.**
- **preeqspin 4** [corresponding to Rspinpreeq 0.17]
  - ✓ **Rspincut 1.**

Rspincut 1, preeqspin n
Rspincut 0.5, preeqspin n
Rspincut 0.25, preeqspin n
Rspincut 1, preeqspin 3
Rspincut 1, preeqspin 4

```
projectile d
element   Nb/Zr/Mo
mass      0
energy    energies
popeps 1.e-12
partable y
#
bins 100
breakupmodel 2
deuteronomp 2
#
Preeqspin 1/3/4
Rspincut  1./ 0.5/ 0.25
#
#
filetotal y
```

analyzed through the comparison of the experimental and TALYS-1.97 activation excitation functions corresponding to **Nb(d,x), ^{nat}Zr(d,x), ^{nat}Mo(d,x)**

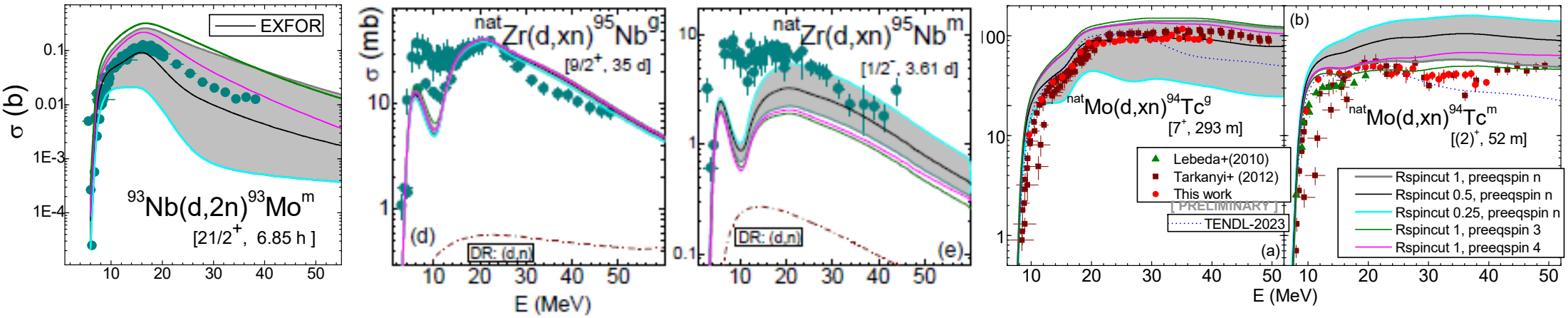

Decreasing I/I_0 ratio, Rspincut, or Rspincutpreeq (preeqspin 4), increases low spin isomeric states population